

Three-flavor Nambu–Jona-Lasinio model at finite isospin chemical potential

Tao Xia,¹ Lianyi He,² and Pengfei Zhuang¹

¹ *Department of Physics, Tsinghua University, Beijing 100084, China*

² *Frankfurt Institute for Advanced Studies, J. W. Goethe University, 60438 Frankfurt am Main, Germany*

(Dated: September 19, 2013)

QCD at finite isospin chemical potential μ_I possesses a positively definite fermion determinant and the lattice simulation can be successfully performed. While the two-flavor effective models may be sufficient to describe the phenomenon of pion condensation, it is interesting to study the roles of the strangeness degree of freedom and the $U_A(1)$ anomaly. In this paper, we present a systematic study of the three-flavor Nambu–Jona-Lasinio model with a Kobayashi-Maskawa-’t Hooft (KMT) term that mimics the $U_A(1)$ anomaly at finite isospin chemical potential. In the mean-field approximation, the model predicts a phase transition from the vacuum to the pion superfluid phase, which takes place at μ_I equal to the pion mass m_π . Due to the $U_A(1)$ anomaly, the strangeness degree of freedom couples to the light quark degrees of freedom and the strange quark effective mass depends on the pion condensate. However, the strange quark condensate and the strange quark effective mass change slightly in the pion superfluid phase, which verifies the validity of the two-flavor models. The effective four-fermion interaction of the Kobayashi-Maskawa-’t Hooft term in the presence of the pion condensation is constructed. Due to the $U_A(1)$ anomaly, the pion condensation generally induces scalar-pseudoscalar interaction. The Bethe-Salpeter equation for the mesonic excitations is established and the meson mass spectra are obtained at finite isospin chemical potential and temperature. Finally, the general expression for the topological susceptibility χ at finite isospin chemical potential μ_I is derived. In contrast to the finite temperature effect which suppresses χ , the isospin density effect leads to an enhancement of χ .

PACS numbers: 11.10.Wx, 12.38.-t, 25.75.Nq

I. INTRODUCTION

Good knowledge of quantum chromodynamics (QCD) at finite temperature and density is important for us to understand a wide range of physical phenomena. To understand the evolution of the early Universe in the first few seconds, we need the nature of the QCD phase transition at temperature $T \sim 170\text{MeV}$ and nearly vanishing baryon density. On the other hand, to understand the physics of compact stars, we need the knowledge of the equation of state and dynamics of QCD matter at high baryon density and low temperature. Lattice simulation of QCD at finite temperature and vanishing density has been successfully performed. However, at large baryon density the lattice simulation has not yet been successfully done due to the sign problem [1]: The fermion determinant is not positively definite in the presence of a nonzero baryon chemical potential μ_B .

To study the nature of strongly interacting matter at finite density, we thus look for some special theories that possess a positively definite fermion determinant. One case is the so-called QCD-like theories at finite baryon density [2], where quarks are in a real or pseudoreal representation of the gauge group, including two-color QCD with quarks in the fundamental representation and QCD with quarks in the adjoint representation. While these theories are not real QCD, they can be simulated on the lattice [3] and may give us some information of real QCD at finite baryon density. Another interesting case is real QCD at finite isospin chemical potential μ_I [4], where the chemical potentials for light u and d quarks have opposite signs and hence the fermion determinant is positively definite. Chiral perturbation theory and other effective models predict a continuous quantum phase transition from the vacuum to the matter phase at μ_I equal to the pion mass m_π [4–

6], in contrast to the finite μ_B case, where the phase transition takes place at μ_B approximately equal to the nucleon mass m_N . This transition has also been verified by lattice simulations of QCD at finite isospin chemical potential [7]. The resulting matter near the quantum phase transition is a dilute Bose condensate of pions with weakly repulsive interactions [8].

The Bose-Einstein condensation (BEC) phenomenon is believed to widely exist in dense strongly interacting matter. For example, pions or kaons can condense in neutron star matter if the electron chemical potential exceeds the effective mass for the pions or kaons [9–12]. However, the condensation of pions and kaons in neutron star matter is rather complicated due to the meson-nucleon interactions in dense nuclear medium. On the other hand, at asymptotically high density, perturbative QCD calculations show that the ground state of dense QCD is a weakly coupled BCS superfluid with the condensation of overlapping Cooper pairs [13]. For QCD at finite isospin density, it is interesting that the dense BCS superfluid and the dilute pion condensate have the same symmetry-breaking pattern and thus are continued with one another [4]. They are both characterized by the nonzero expectation value $\langle \bar{u}i\gamma_5 d \rangle \neq 0$. In condensed matter physics, this phenomenon was first discussed by Eagles [14] and Leggett [15] and is now called BEC-BCS crossover [16]. The BEC-BCS crossover in dense relativistic systems as well as in dense QCD matter has been extensively studied in recent years [17, 18].

While the two-flavor effective models of QCD may be sufficient to describe the phenomenon of pion condensation at finite isospin density, it is interesting to study the roles of the strangeness degree of freedom and the $U_A(1)$ anomaly. The Nambu–Jona-Lasinio (NJL) model [19] with quarks as elementary blocks, which describes well the mechanism of chiral symmetry breaking and low-energy phenomenology of the QCD vacuum, is generally believed to work at low and

moderate temperatures and densities [20]. The pion and kaon condensation in the three-flavor NJL model without $U_A(1)$ anomaly has been studied by Barducci *et al.* [21] and by Warringa *et al.* [22]. It is well known that the Kobayashi-Maskawa-'t Hooft (KMT) term, which mimics the $U_A(1)$ anomaly in the NJL model, is crucial to describe the $\eta - \eta'$ mass splitting and therefore the meson spectra of QCD [20]. Therefore, to study the meson spectra at finite isospin chemical potential, we need to consider the KMT term.

The Lagrangian density of the three-flavor Nambu–Jona-Lasinio model is given by [20]

$$\mathcal{L}_{\text{NJL}} = \bar{\psi}(i\gamma_\mu\partial^\mu - \hat{m}_0)\psi + \mathcal{L}_S + \mathcal{L}_{\text{KMT}}, \quad (1)$$

where $\psi = (u, d, s)^T$ denotes the quark field and \hat{m}_0 represents the current quark mass matrix $\hat{m}_0 = \text{diag}(m_u, m_d, m_s)$. In this work we assume isospin symmetry, i.e., $m_u = m_d \equiv m_l$. The four-fermion interaction term \mathcal{L}_S is given by

$$\mathcal{L}_S = G \sum_{\alpha=0}^{N_f^2-1} [(\bar{\psi}\lambda_\alpha\psi)^2 + (\bar{\psi}i\gamma_5\lambda_\alpha\psi)^2], \quad (2)$$

where $N_f = 3$ for our three-flavor model, λ_α are the Gell-Mann matrices in flavor space with $\lambda_0 = \sqrt{2/3}\mathbf{I}$, and G is the coupling constant. This term represents the interactions with flavor $U_L(3) \times U_R(3)$ symmetry in scalar and pseudoscalar channels. However, in real QCD the flavor symmetry (in the chiral limit $m_l = m_s = 0$) is broken down to $SU_L(3) \times SU_R(3) \times U_B(1)$ due to the $U_A(1)$ anomaly. In the NJL model, this can be realized by adding the so-called KMT term \mathcal{L}_{KMT} to the Lagrangian density. It reads

$$\mathcal{L}_{\text{KMT}} = -K [\det\bar{\psi}(1 + \gamma_5)\psi + \det\bar{\psi}(1 - \gamma_5)\psi]. \quad (3)$$

The KMT term contains six-fermion interactions in the three-flavor case. The coupling constant G and the $U_A(1)$ breaking strength K can be determined by the vacuum phenomenology of QCD. It has been shown that the three-flavor NJL model with KMT term describes well the meson spectra of QCD, especially the $\eta - \eta'$ mass splitting [20]. In this paper we shall present a systematic study of this model at finite isospin chemical potential μ_I .

The above three-flavor NJL model also enables us to study the behavior of the topological susceptibility χ at finite isospin chemical potential μ_I . The topological susceptibility χ is a fundamental correlation function in QCD and is the key to understanding much of the distinctive dynamics in the $U_A(1)$ channel. The general expression of χ to the leading order in the $1/N_c$ expansion at finite temperature and vanishing chemical potentials for the three-flavor NJL model has been derived by Fukushima *et al.* [23]. It was shown that the temperature effect suppresses the topological susceptibility χ . On the other hand, the finite-temperature behavior of the topological susceptibility can also be determined by lattice QCD [24]. Therefore, the temperature dependence of the $U_A(1)$ anomaly strength K in the NJL model may be determined by using the lattice data. A relatively small K at large temperature may signal an effective restoration of the $U_A(1)$ anomaly. In this paper we will calculate the topological susceptibility χ at finite isospin chemical potential μ_I . Since we have no available

lattice data for χ at finite μ_I , we will treat K as a constant. While one may expect a similar suppression of χ as in the case at finite temperature, we find instead a clear enhancement at finite isospin density. Our model prediction may be tested by future lattice simulations, and the μ_I dependence of the $U_A(1)$ anomaly strength K may also be determined by using our expression of χ .

The paper is organized as follows. In Sec. II, we study the three-flavor NJL model in the mean-field approximation, which enables us to obtain the chiral and pion condensates, the phase diagram, and the equation of state at finite isospin chemical potential. In Sec. III, we construct the effective four-fermion interaction of the KMT term in the presence of the pion condensation. Using the effective four-fermion interaction, the mesonic excitations at finite isospin chemical potential are studied within the random-phase approximation. The topological susceptibility at finite isospin chemical potential is investigated in Sec. IV. We summarize in Sec. V.

II. MESON CONDENSATION IN MEAN-FIELD APPROXIMATION

To study the three-flavor NJL model at finite chemical potentials and temperature, we introduce the chemical potential matrix $\hat{\mu} = \text{diag}(\mu_u, \mu_d, \mu_s)$, where

$$\mu_u = \frac{\mu_B}{3} + \frac{\mu_I}{2}, \quad \mu_d = \frac{\mu_B}{3} - \frac{\mu_I}{2}, \quad \mu_s = \frac{\mu_B}{3} - \mu_s. \quad (4)$$

Here μ_B , μ_I and μ_s are referred to as the baryon chemical potential, isospin chemical potential, and strangeness chemical potential, respectively. At finite temperature and chemical potentials, the partition function of the NJL model reads

$$Z(T, \mu_B, \mu_I, \mu_s) = \int [d\bar{\psi}][d\psi] \exp \left[- \int_0^\beta d\tau \int d^3\mathbf{x} \mathcal{L} \right], \quad (5)$$

where $\mathcal{L} = \mathcal{L}_{\text{NJL}} + \bar{\psi}\hat{\mu}\gamma_0\psi$ and β is the inverse of the temperature T .

However, the partition function $Z(T, \mu_B, \mu_I, \mu_s)$ cannot be evaluated precisely. The standard approach for the NJL model is to replace some composite (meson) fields by their expectation values and therefore replace the Lagrangian density \mathcal{L} by its mean-field approximation \mathcal{L}_{mf} [20]. To this end, we first introduce the chiral condensates for the three quark flavors,

$$\sigma_u = \langle \bar{u}u \rangle, \quad \sigma_d = \langle \bar{d}d \rangle, \quad \sigma_s = \langle \bar{s}s \rangle. \quad (6)$$

It is well known that these condensates are nonzero in the vacuum, corresponding to the spontaneous chiral symmetry breaking of the QCD vacuum in the chiral limit $m_l = m_s = 0$. At finite isospin and strangeness chemical potentials, some pseudoscalar condensates may arise, corresponding to the condensation of pions and kaons. Therefore, we also introduce the following pseudoscalar condensates:

$$\phi_{ud} = 2\langle \bar{u}i\gamma_5 d \rangle, \quad \phi_{us} = 2\langle \bar{u}i\gamma_5 s \rangle, \quad \phi_{ds} = 2\langle \bar{d}i\gamma_5 s \rangle. \quad (7)$$

A nonzero isospin chemical potential μ_I breaks the isospin symmetry $SU_I(2)$ down to $U_I(1)$ with generator I_3 . The

nonzero expectation value of the pseudoscalar condensate ϕ_{ud} spontaneously breaks the residual $U_1(1)$ symmetry, corresponding to Bose-Einstein condensation of charged pions. On the other hand, if $\phi_{us} \neq 0$ or $\phi_{ds} \neq 0$, the $U_S(1)$ symmetry corresponding to the conservation of strangeness becomes spontaneously broken, corresponding to the Bose-Einstein condensation of kaons.

The general form of the mean-field Lagrangian density \mathcal{L}_{mf} takes the form

$$\mathcal{L}_{\text{mf}} = \bar{\psi}(\mathcal{S}_0^{-1} + \Sigma)\psi - \mathcal{V} \quad (8)$$

where $\mathcal{S}_0^{-1} = i\gamma_\mu \partial^\mu + \hat{\mu}\gamma_0 - \hat{m}_0$, Σ is the quark self-energy in the mean-field approximation, and \mathcal{V} is the condensation energy that is independent of the quark fields. In the presence of pion and kaon condensation, the self-energy is not diagonal in flavor and can be expressed as

$$\Sigma = \begin{pmatrix} \Sigma_{uu} & \Sigma_{ud} & \Sigma_{us} \\ \Sigma_{du} & \Sigma_{dd} & \Sigma_{ds} \\ \Sigma_{su} & \Sigma_{sd} & \Sigma_{ss} \end{pmatrix}. \quad (9)$$

Accordingly, the quark propagator \mathcal{S} is also not diagonal. To get the mean-field Lagrangian density \mathcal{L}_{mf} , we replace any composite field operator \mathcal{O} by $\mathcal{O} = \langle \mathcal{O} \rangle + \delta$ and keep only the lowest order in the fluctuation δ . For the KMT term \mathcal{L}_{KMT} , it contains six-fermion interaction. The determinant is taken over the flavor space. We have

$$\det \bar{\psi} \Gamma \psi = \det \begin{pmatrix} \bar{u} \Gamma u & \bar{u} \Gamma d & \bar{u} \Gamma s \\ \bar{d} \Gamma u & \bar{d} \Gamma d & \bar{d} \Gamma s \\ \bar{s} \Gamma u & \bar{s} \Gamma d & \bar{s} \Gamma s \end{pmatrix}, \quad (10)$$

where $\Gamma = 1 \pm \gamma_5$. Therefore, in the presence of meson condensates ϕ_{ud} , ϕ_{us} , and ϕ_{ds} , the off-diagonal components contribute and the mean-field approximation of the KMT term should be taken carefully.

After some tedious calculations, we obtain the expression for the condensation energy,

$$\mathcal{V} = 2G(\sigma_u^2 + \sigma_d^2 + \sigma_s^2) + G(|\phi_{ud}|^2 + |\phi_{us}|^2 + |\phi_{ds}|^2) - 4K\sigma_u\sigma_d\sigma_s - K(|\phi_{ud}|^2\sigma_s + |\phi_{us}|^2\sigma_d + |\phi_{ds}|^2\sigma_u). \quad (11)$$

With the result of the self-energy, the inverse of the quark propagator \mathcal{S} can be expressed as

$$\mathcal{S}^{-1} = \mathcal{S}_0^{-1} + \Sigma = \begin{pmatrix} i\gamma^\mu \partial_\mu - M_u & \Sigma_{ud} & \Sigma_{us} \\ \Sigma_{du} & i\gamma^\mu \partial_\mu - M_d & \Sigma_{ds} \\ \Sigma_{su} & \Sigma_{sd} & i\gamma^\mu \partial_\mu - M_s \end{pmatrix} + \hat{\mu}\gamma_0, \quad (12)$$

where the effective quark masses are defined as

$$\begin{aligned} M_u &= m_u - 4G\sigma_u + 2K\sigma_d\sigma_s + \frac{K}{2}|\phi_{ds}|^2, \\ M_d &= m_d - 4G\sigma_d + 2K\sigma_u\sigma_s + \frac{K}{2}|\phi_{us}|^2, \\ M_s &= m_s - 4G\sigma_s + 2K\sigma_u\sigma_d + \frac{K}{2}|\phi_{ud}|^2 \end{aligned} \quad (13)$$

and the off-diagonal components of the self-energy read

$$\begin{aligned} \Sigma_{ud} &= \Sigma_{du}^* = i\gamma_5(2G - K\sigma_s)\phi_{ud}^* + \frac{K}{2}\phi_{us}^*\phi_{ds}, \\ \Sigma_{us} &= \Sigma_{su}^* = i\gamma_5(2G - K\sigma_d)\phi_{us}^* + \frac{K}{2}\phi_{ud}^*\phi_{ds}^*, \\ \Sigma_{ds} &= \Sigma_{sd}^* = i\gamma_5(2G - K\sigma_u)\phi_{ds}^* + \frac{K}{2}\phi_{ud}^*\phi_{us}^*. \end{aligned} \quad (14)$$

An alternative way for calculating the mean-field approximation to the self-energy Σ is to Wick-contract all possible pairs of creation and destruction field operators in the Lagrangian, so that only two remain “alive” as field operators. To the lowest order in the $1/N_c$ expansion, the result from this method should be consistent with the mean-field approximation. In the absence of meson condensates, the above expressions recover the well-known result for the three-flavor NJL model [20]. However, in the presence of meson condensates, we find that they contribute to the effective quark masses $M_i (i = u, d, s)$ due to the $U_A(1)$ anomaly.

Having obtained the mean-field approximation of the Lagrangian density, we can work out the path integral by replacing \mathcal{L} with \mathcal{L}_{mf} . The mean-field approximation to the thermodynamic potential reads

$$\Omega_{\text{mf}} = \mathcal{V} - \frac{1}{\beta V} \text{Tr} \ln \mathcal{S}^{-1}. \quad (15)$$

In general, the physical values of the condensates can be obtained by minimizing the thermodynamic potential at given temperature and chemical potentials. In this work, we focus on the case $\mu_B = \mu_S = 0$ and $\mu_l \neq 0$. In this case, we have $\sigma_u = \sigma_d \equiv \sigma_l$ and $\phi_{us} = \phi_{ds} = 0$ (no kaon condensation). The thermodynamic potential can be analytically evaluated as

$$\begin{aligned} \Omega_{\text{mf}} &= G(4\sigma_l^2 + 2\sigma_s^2 + |\phi_{ud}|^2) - K\sigma_s(4\sigma_l^2 + |\phi_{ud}|^2) \\ &\quad - 2N_c \int \frac{d^3\mathbf{k}}{(2\pi)^3} (E_{\mathbf{k}}^+ + E_{\mathbf{k}}^- + E_{\mathbf{k}}^s) \\ &\quad - 4N_c T \int \frac{d^3\mathbf{k}}{(2\pi)^3} \left[\ln(1 + e^{-\beta E_{\mathbf{k}}^+}) \right. \\ &\quad \left. + \ln(1 + e^{-\beta E_{\mathbf{k}}^-}) + \ln(1 + e^{-\beta E_{\mathbf{k}}^s}) \right], \end{aligned} \quad (16)$$

where the dispersions are defined as

$$\begin{aligned} E_{\mathbf{k}}^\pm &= \sqrt{(E_{\mathbf{k}}^l \pm \mu_l/2)^2 + |\Delta|^2}, \\ E_{\mathbf{k}}^l &= \sqrt{\mathbf{k}^2 + M_l^2}, \\ E_{\mathbf{k}}^s &= \sqrt{\mathbf{k}^2 + M_s^2}. \end{aligned} \quad (17)$$

Here the effective quark masses for light and strange quarks have been reduced to

$$\begin{aligned} M_l &= m_q - 4G\sigma_l + 2K\sigma_l\sigma_s, \\ M_s &= m_s - 4G\sigma_s + 2K\sigma_l^2 + \frac{K}{2}|\phi_{ud}|^2, \end{aligned} \quad (18)$$

and the quantity Δ is given by

$$\Delta = (2G - K\sigma_s)\phi_{ud}. \quad (19)$$

Since the thermodynamic potential depends only on $|\phi_{ud}|^2$, we can set ϕ_{ud} and Δ to be real values without loss of generality. This is related to the spontaneous breaking of the $U_1(1)$ symmetry, which means the phase of the order parameter ϕ_{ud} can be chosen arbitrarily.

In the momentum space, the quark propagator $S(k)$ takes the form

$$S(k) = \begin{pmatrix} S_{uu}(k) & S_{ud}(k) & 0 \\ S_{du}(k) & S_{dd}(k) & 0 \\ 0 & 0 & S_s(k) \end{pmatrix}, \quad (20)$$

where $k = (i\omega_n, \mathbf{k})$ with $\omega_n = (2n+1)\pi T$ (n integer) being the fermion Matsubara frequency. The nonzero components can be analytically evaluated as [25]

$$\begin{aligned} S_{uu}(k) &= \frac{i\omega_n + \xi_{\mathbf{k}}^-}{(i\omega_n)^2 - (E_{\mathbf{k}}^-)^2} \Lambda_+^l \gamma_0 + \frac{i\omega_n - \xi_{\mathbf{k}}^+}{(i\omega_n)^2 - (E_{\mathbf{k}}^+)^2} \Lambda_-^l \gamma_0, \\ S_{dd}(k) &= \frac{i\omega_n - \xi_{\mathbf{k}}^-}{(i\omega_n)^2 - (E_{\mathbf{k}}^-)^2} \Lambda_-^l \gamma_0 + \frac{i\omega_n + \xi_{\mathbf{k}}^+}{(i\omega_n)^2 - (E_{\mathbf{k}}^+)^2} \Lambda_+^l \gamma_0, \\ S_{ud}(k) &= \frac{i\Delta}{(i\omega_n)^2 - (E_{\mathbf{k}}^-)^2} \Lambda_+^l \gamma_5 + \frac{i\Delta}{(i\omega_n)^2 - (E_{\mathbf{k}}^+)^2} \Lambda_-^l \gamma_5, \\ S_{du}(k) &= \frac{i\Delta}{(i\omega_n)^2 - (E_{\mathbf{k}}^-)^2} \Lambda_-^l \gamma_5 + \frac{i\Delta}{(i\omega_n)^2 - (E_{\mathbf{k}}^+)^2} \Lambda_+^l \gamma_5, \\ S_s(k) &= \frac{1}{i\omega_n - E_{\mathbf{k}}^s} \Lambda_+^s \gamma_0 + \frac{1}{i\omega_n + E_{\mathbf{k}}^s} \Lambda_-^s \gamma_0, \end{aligned} \quad (21)$$

where $\xi_{\mathbf{k}}^\pm = E_{\mathbf{k}}^l \pm \mu_l/2$ and the energy projectors Λ_\pm^l and Λ_\pm^s are defined as

$$\begin{aligned} \Lambda_\pm^l &= \frac{1}{2} \left[1 \pm \frac{\gamma_0(\boldsymbol{\gamma} \cdot \mathbf{k} + M_l)}{E_{\mathbf{k}}^l} \right], \\ \Lambda_\pm^s &= \frac{1}{2} \left[1 \pm \frac{\gamma_0(\boldsymbol{\gamma} \cdot \mathbf{k} + M_s)}{E_{\mathbf{k}}^s} \right]. \end{aligned} \quad (22)$$

The gap equations that determine the physical values of the chiral and pion condensates can be obtained by minimizing the thermodynamic potential Ω_{mf} . Self-consistently, they can also be derived from the Green's function relations. We have

$$\begin{aligned} \sigma_l &= \frac{N_c}{\beta} \sum_n \int \frac{d^3\mathbf{k}}{(2\pi)^3} \text{Tr}_D S_{uu}(k) \\ &= \frac{N_c}{\beta} \sum_n \int \frac{d^3\mathbf{k}}{(2\pi)^3} \text{Tr}_D S_{dd}(k), \\ \sigma_s &= \frac{N_c}{\beta} \sum_n \int \frac{d^3\mathbf{k}}{(2\pi)^3} \text{Tr}_D S_s(k), \\ \phi_{ud} &= 2 \frac{N_c}{\beta} \sum_n \int \frac{d^3\mathbf{k}}{(2\pi)^3} \text{Tr}_D [S_{du}(k) i\gamma_5], \end{aligned} \quad (23)$$

where the trace runs only in the spin space. Finally, we get the

explicit expressions of the gap equations

$$\begin{aligned} \sigma_s &= -2N_c M_s \int \frac{d^3\mathbf{k}}{(2\pi)^3} \frac{1 - 2f(E_{\mathbf{k}}^s)}{E_{\mathbf{k}}^s}, \\ \sigma_l &= -N_c M_l \int \frac{d^3\mathbf{k}}{(2\pi)^3} \frac{1}{E_{\mathbf{k}}^l} \sum_{\alpha=\pm} \frac{\xi_{\mathbf{k}}^\alpha}{E_{\mathbf{k}}^\alpha} (1 - 2f(E_{\mathbf{k}}^\alpha)), \\ \phi_{ud} &= 2N_c \Delta \int \frac{d^3\mathbf{k}}{(2\pi)^3} \sum_{\alpha=\pm} \frac{1 - 2f(E_{\mathbf{k}}^\alpha)}{E_{\mathbf{k}}^\alpha}, \end{aligned} \quad (24)$$

where $f(E) = 1/(e^{\beta E} + 1)$ is the Fermi-Dirac distribution.

Now we turn to numerical results. The NJL model is non-renormalizable and we introduce an ultraviolet cutoff Λ for the three-momentum to regularize the divergent integrals. The model therefore has five parameters, the current quark masses m_l and m_s , the coupling constant G , the anomaly coupling K , and the cutoff Λ . For the light quark mass, we choose $m_l = 5.5\text{MeV}$. The others can be determined by recovering the well-measured vacuum phenomenology. Here we employ the pion decay constant and the masses of the pion, kaon, and the η' meson. The data we adopted are $f_\pi = 92.4$, $m_\pi = 135.0$, $m_K = 497.7$, and $m_{\eta'} = 957.8\text{MeV}$. The model parameters obtained by fitting these data are $m_l = 5.5$, $m_s = 140.7$, $\Lambda = 602.3\text{MeV}$, $G\Lambda^2 = 1.835$, and $K\Lambda^5 = 12.36$ [26]. Such a parameter set leads to the quark chiral condensate $\langle \bar{l}l \rangle_0 = -(241.9\text{MeV})^3$ and $\langle \bar{s}s \rangle_0 = -(257.7\text{MeV})^3$ and the constituent quark masses $M_l = 367.7$ and $M_s = 549.5\text{MeV}$.

A. Condensates and phase diagram

In Fig. 1 we show the behavior of the chiral and pion condensates with increasing temperature T at vanishing isospin chemical potential. In this case, pion condensation does not arise. The system undergoes a crossover from the low-temperature hadronic matter to the high-temperature quark matter. The results for the chiral condensates shown here are consistent with those reported in the previous studies [26, 27].

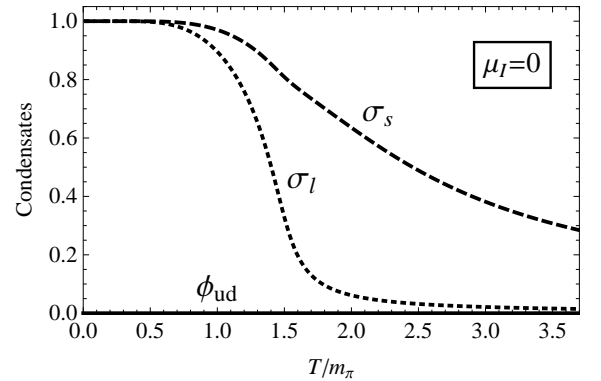


FIG. 1. The chiral and pion condensates as functions of the temperature T at vanishing isospin chemical potential $\mu_l = 0$. σ_l and ϕ_{ud} are scaled by $\langle \bar{l}l \rangle_0$ and $2\langle \bar{l}l \rangle_0$, respectively, and σ_s is scaled by $\langle \bar{s}s \rangle_0$. In the following we use the same quantities to scale the chiral and pion condensates.

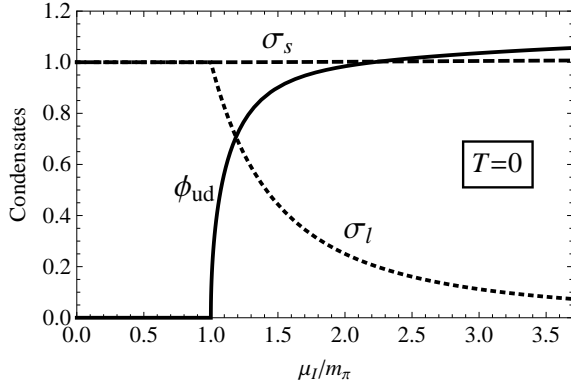


FIG. 2. The chiral and pion condensates as functions of the isospin chemical potential μ_I at zero temperature.

We are most interested in the case of zero temperature and finite isospin chemical potential. Since the charged pions (π^\pm) are the lightest mesons that carry isospin quantum number, we expect that they get condensed as long as the isospin chemical potential μ_I exceeds a critical value. Without loss of generality, we study the case $\mu_I > 0$. Solving the coupled gap equations, we obtain the evolution of the chiral and pion condensates with increasing isospin chemical potential, as shown in Fig. 2. We find that the onset of pion condensation is located precisely at $\mu_I = m_\pi$, as has been shown analytically in the two-flavor NJL model [6]. In the three-flavor model, this can also be shown explicitly. In the regime $|\mu_I| < m_\pi$, the chiral condensates keep their values in the vacuum, which means that the system stays in the vacuum for $|\mu_I| < m_\pi$ and no isospin charge is excited. At the onset of pion condensation, we have from the gap equations

$$1 = 2N_c(2G - K\sigma_s) \int \frac{d^3\mathbf{k}}{(2\pi)^3} \frac{2E_{\mathbf{k}}^l}{(E_{\mathbf{k}}^l)^2 - \mu_I^2/4}. \quad (25)$$

This equation coincides with the mass equation for the pion in the vacuum and gives precisely $\mu_I = m_\pi$.

When the isospin chemical potential μ_I exceeds the critical value m_π , the light quark chiral condensate σ_l decreases significantly and the isospin density is generated due to the appearance of condensed pions. The behavior of the pion condensate ϕ_{ud} and the light quark chiral condensate σ_l is similar to that found in the two-flavor model [6]. Let us now focus on the roles of the strangeness and the $U_A(1)$ anomaly. In the absence of the $U_A(1)$ anomaly, i.e., $K = 0$, the gap equation for the strange quark chiral condensate σ_s decouples from the other two equations. Therefore, the strangeness degree of freedom has nothing to do with the pion condensation for $K = 0$. The strange quark chiral condensate σ_s just keeps its vacuum value no matter how large μ_I is. However, in the presence of the $U_A(1)$ anomaly, the strange quark chiral condensate σ_s couples to the other condensates through the non-vanishing anomaly strength K . Therefore, the strange quark chiral condensate should change in the pion condensed phase. However, from its behavior in Fig. 2, we find that its change is very slight. In Fig. 3, we show a zoom plot for the strange

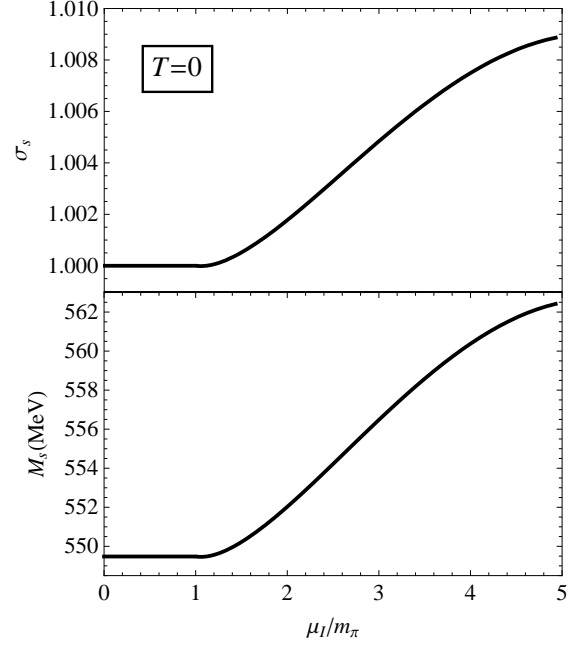


FIG. 3. A zoom look at the behavior of the strange quark chiral condensate σ_s and the strange quark effective mass M_s at finite isospin chemical potential.

quark chiral condensate σ_s . It starts to increase at the onset of pion condensation. However, the value is only increased by about 1% at $\mu_I = 5m_\pi$. The behavior of the strange quark effective mass M_s is also shown in Fig. 3. It is increased by about 12 MeV at $\mu_I = 5m_\pi$. Therefore, our studies of the three-flavor NJL model verify the validity of the two-flavor models in the description of pion condensation.

At finite temperature, the pion condensate gets melted. In general there exists a phase transition from the pion superfluid phase to the normal phase with $\phi_{ud} = 0$. In the present model, we find this transition is of second order. In Fig. 4, we show the finite-temperature behavior of the chiral and pion condensates at $\mu_I > m_\pi$. The temperature effect, while reduces the pion condensate ϕ_{ud} and the strange quark chiral condensate σ_s , enhances the light quark chiral condensate σ_q in the superfluid domain $T < T_c$. At high temperature, all condensates are suppressed by the temperature effect.

In Fig. 5, we show the phase diagram of the present model in the T - μ_I plane. The phase boundary between the superfluid phase and the normal phase is determined by the line where the pion condensate ϕ_{ud} vanishes. For the normal phase in the domain $\mu_I < m_\pi$, there exists a crossover from the low-temperature hadronic matter to the high-temperature quark matter that we do not show explicitly. In the superfluid phase we also expect a BEC-BCS crossover from pion condensation to quark-antiquark condensation. Near the onset of pion condensation $\mu_I = m_\pi$, the system can be identified as a dilute Bose-Einstein condensate of weakly interacting pions. However, at large isospin density, the pions no longer remain tightly bound bosons, and the system becomes a BCS super-

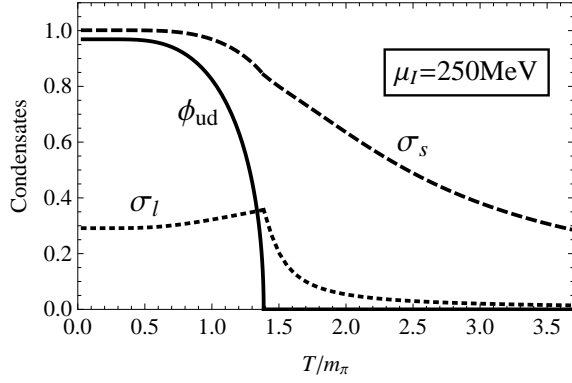


FIG. 4. The chiral and pion condensates as functions of the temperature T at fixed isospin chemical potential $\mu_l = 250$ MeV.

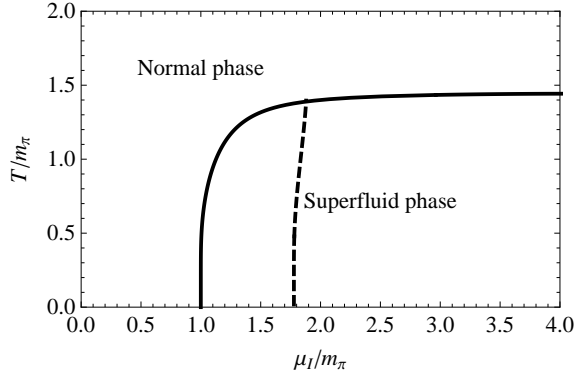


FIG. 5. Phase diagram of the three-flavor NJL model in the $T-\mu_l$ plane. The normal and superfluid phases correspond to the phases with vanishing and nonvanishing pion condensates, respectively. The black dashed line denotes the BEC-BCS crossover from pion to quark-antiquark condensation.

fluid with condensation of quark-antiquark pairs (but with the same quantum number of pions). According to the spirit of the BEC-BCS crossover [16], the crossover can be estimated by studying the fermionic excitation spectrum. Here we focus on the excitation spectrum $E_{\mathbf{k}}^-$ [17, 18]. Its minimum remains at $\mathbf{k} = 0$ for $M_l > \mu_l/2$ but shifts to nonzero momentum if $M_l < \mu_l/2$. The BEC-BCS crossover line can be estimated by the condition $M_l(\mu_l) = \mu_l/2$. This line is shown in Fig. 5. A clear picture the BEC-BCS crossover can be shown by studying the behavior of the pions above the superfluid critical temperature T_c . In the BEC domain, the pions are bound bosons above T_c . However, they become loose resonances at the BCS side.

B. Equation of state

In the final part of the section, we study the equation of state of the isospin matter. Here we focus on the zero temperature case.

In Fig. 6, we show the isospin density n_l as a function of the isospin chemical potential μ_l . In the mean-field approxi-

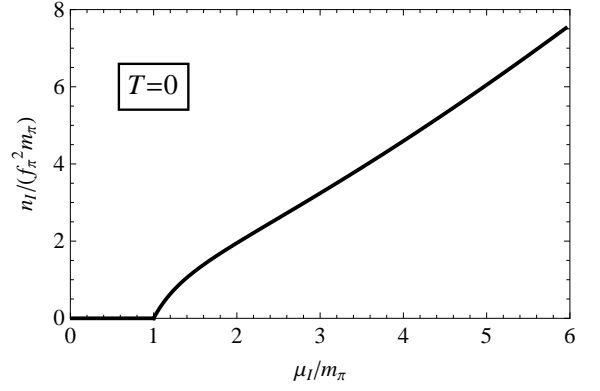


FIG. 6. The isospin density n_l (scaled by $f_\pi^2 m_\pi$) as a function of the isospin chemical potential μ_l .

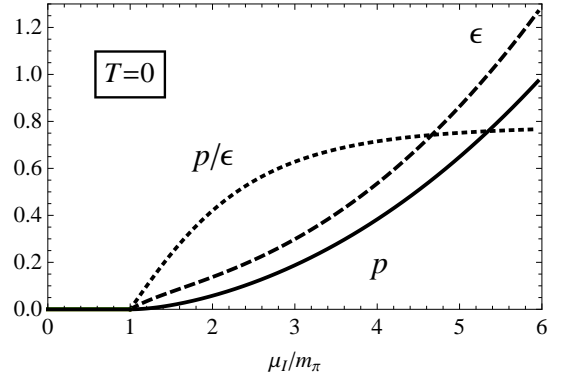


FIG. 7. The pressure and energy densities, p and ϵ , as functions of the isospin chemical potential μ_l . They have been scaled by the quantity $20f_\pi^2 m_\pi^2$. The ratio p/ϵ is also shown.

mation, the isospin density n_l reads

$$n_l = N_c \int \frac{d^3\mathbf{k}}{(2\pi)^3} \left(\frac{\xi_{\mathbf{k}}^+}{E_{\mathbf{k}}^+} - \frac{\xi_{\mathbf{k}}^-}{E_{\mathbf{k}}^-} \right). \quad (26)$$

From this expression, we see clearly that the isospin density remains zero for the regime $|\mu_l| < m_\pi$, and it becomes nonzero in the superfluid phase. Near the onset of pion condensation, the numerical result agrees well with that predicted by the chiral perturbation theory,

$$n_l \simeq f_\pi^2 \mu_l \left(1 - \frac{m_\pi^4}{\mu_l^4} \right). \quad (27)$$

However, at large isospin chemical potential, this behavior no longer holds, since the system undergoes BEC-BCS crossover and is no longer Bose-Einstein condensate of weakly interacting pions.

In Fig. 7 the pressure p and the energy density ϵ are shown as functions of the isospin chemical potential. They keep vanishing in the regime $|\mu_l| < m_\pi$, and arise in the superfluid phase due to the appearance of condensed pions. In Fig. 8, we show the energy density ϵ scaled by its Stefan-Boltzmann limit,

$$\epsilon_{\text{SB}} = \frac{N_f N_c}{4\pi^2} \left(\frac{\mu_l}{2} \right)^4. \quad (28)$$

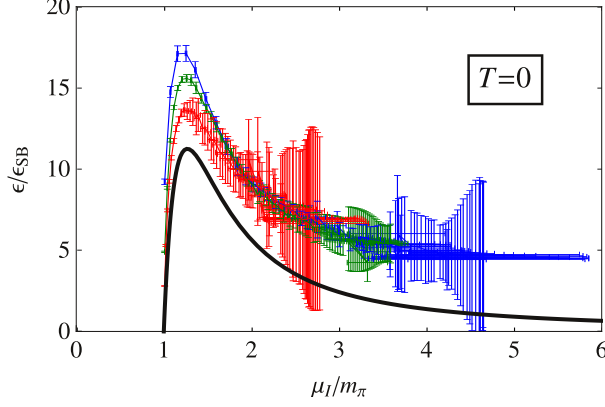


FIG. 8. (color online). The energy density ϵ scaled by its Stefan-Boltzmann limit as a function of the isospin chemical potential μ_I . The colorful data are taken from recent lattice simulation [28]. Different colors correspond to different lattice spatial spacings used in the simulation.

The result from recent lattice simulation [28] with a larger pion mass $m_\pi \sim 390\text{MeV}$ is also shown as a comparison. We find that the scaled energy density $\epsilon/\epsilon_{\text{SB}}$ shows a peak near the onset of the pion condensation (at $\mu_I \simeq 1.3m_\pi$), which is consistent with the lattice result.

III. MESONIC EXCITATIONS IN THE RANDOM-PHASE APPROXIMATION

In the spirit of the Nambu–Jona-Lasinio model, the mesons are regarded as collective excitations [19, 20]. The meson propagator, to the leading order in $1/N_c$, can be constructed by an infinite sum of the quark-antiquark ring diagrams associated with the four-fermion interaction, or the so-called random-phase approximation that is recognized to be a geometric progression. However, in the present three-flavor model, the interaction terms contains not only four-fermion interaction but also six-fermion interaction (due to the KMT term). Therefore, to study the mesonic excitations at finite isospin chemical potential and temperature, we should first construct an effective Lagrangian with only effective four-fermion interactions.

Let us now construct an effective four-fermion interaction $\mathcal{L}_{\text{KMT}}^{4f}$ for the KMT term. We expect that we obtain the same self-energy Σ after taking the mean-field approximation for $\mathcal{L}_{\text{KMT}}^{4f}$. We do this by contracting out one quark and one antiquark field operator, such that an effective four-fermion interaction is remaining. Unlike the procedure for the vacuum case where $\phi_{ud} = 0$, here we should take care of the effect of the pion condensate ϕ_{ud} that leads to scalar-pseudoscalar mixing. After a tedious calculation, we obtain

$$\mathcal{L}_{\text{KMT}}^{4f} = \mathcal{L}_{\text{KMT}}^s + \mathcal{L}_{\text{KMT}}^p + \mathcal{L}_{\text{KMT}}^{\text{sp}}, \quad (29)$$

where $\mathcal{L}_{\text{KMT}}^s$ is the scalar interaction part,

$$\begin{aligned} \mathcal{L}_{\text{KMT}}^s = & -\frac{K}{3}(2\sigma_l + \sigma_s)(\bar{\psi}\lambda_0\psi)^2 + \frac{K}{2}\sigma_s(\bar{\psi}\lambda_3\psi)^2 \\ & + \frac{K}{6}(4\sigma_l - \sigma_s)(\bar{\psi}\lambda_8\psi)^2 \\ & + \frac{\sqrt{2}}{3}K(\sigma_l - \sigma_s)(\bar{\psi}\lambda_0\psi)(\bar{\psi}\lambda_8\psi) \\ & + K\sigma_s(\bar{\psi}\lambda_1^-\psi)(\bar{\psi}\lambda_1^+\psi) \\ & + K\sigma_l(\bar{\psi}\lambda_4^-\psi)(\bar{\psi}\lambda_4^+\psi) \\ & + K\sigma_l(\bar{\psi}\lambda_6^-\psi)(\bar{\psi}\lambda_6^+\psi), \end{aligned} \quad (30)$$

$\mathcal{L}_{\text{KMT}}^p$ is the pseudoscalar interaction part,

$$\begin{aligned} \mathcal{L}_{\text{KMT}}^p = & \frac{K}{3}(2\sigma_l + \sigma_s)(\bar{\psi}i\gamma_5\lambda_0\psi)^2 - \frac{K}{2}\sigma_s(\bar{\psi}i\gamma_5\lambda_3\psi)^2 \\ & - \frac{K}{6}(4\sigma_l - \sigma_s)(\bar{\psi}i\gamma_5\lambda_8\psi)^2 \\ & - \frac{\sqrt{2}}{3}K(\sigma_l - \sigma_s)(\bar{\psi}i\gamma_5\lambda_0\psi)(\bar{\psi}i\gamma_5\lambda_8\psi) \\ & - K\sigma_s(\bar{\psi}i\gamma_5\lambda_1^-\psi)(\bar{\psi}i\gamma_5\lambda_1^+\psi) \\ & - K\sigma_l(\bar{\psi}i\gamma_5\lambda_4^-\psi)(\bar{\psi}i\gamma_5\lambda_4^+\psi) \\ & - K\sigma_l(\bar{\psi}i\gamma_5\lambda_6^-\psi)(\bar{\psi}i\gamma_5\lambda_6^+\psi), \end{aligned} \quad (31)$$

and $\mathcal{L}_{\text{KMT}}^{\text{sp}}$ is the scalar-pseudoscalar interaction part,

$$\begin{aligned} \mathcal{L}_{\text{KMT}}^{\text{sp}} = & -\frac{\sqrt{3}}{6}K\phi_{ud}^*[(\bar{\psi}i\gamma_5\lambda_0\psi)(\bar{\psi}\lambda_1^+\psi) + (\bar{\psi}\lambda_0\psi)(\bar{\psi}i\gamma_5\lambda_1^+\psi)] \\ & - \frac{\sqrt{3}}{6}K\phi_{ud}[(\bar{\psi}i\gamma_5\lambda_0\psi)(\bar{\psi}\lambda_1^-\psi) + (\bar{\psi}\lambda_0\psi)(\bar{\psi}i\gamma_5\lambda_1^-\psi)] \\ & + \frac{K}{\sqrt{6}}\phi_{ud}^*[(\bar{\psi}i\gamma_5\lambda_1^+\psi)(\bar{\psi}\lambda_8\psi) + (\bar{\psi}\lambda_1^+\psi)(\bar{\psi}i\gamma_5\lambda_8\psi)] \\ & + \frac{K}{\sqrt{6}}\phi_{ud}[(\bar{\psi}i\gamma_5\lambda_1^-\psi)(\bar{\psi}\lambda_8\psi) + (\bar{\psi}\lambda_1^-\psi)(\bar{\psi}i\gamma_5\lambda_8\psi)] \\ & + \frac{K}{2}\phi_{ud}^*[(\bar{\psi}\lambda_6^-\psi)(\bar{\psi}i\gamma_5\lambda_4^+\psi) + (\bar{\psi}i\gamma_5\lambda_6^-\psi)(\bar{\psi}\lambda_4^+\psi)] \\ & + \frac{K}{2}\phi_{ud}[(\bar{\psi}\lambda_6^+\psi)(\bar{\psi}i\gamma_5\lambda_4^-\psi) + (\bar{\psi}i\gamma_5\lambda_6^+\psi)(\bar{\psi}\lambda_4^-\psi)]. \end{aligned} \quad (32)$$

Here we have defined

$$\begin{aligned} \lambda_1^\pm &= \frac{1}{\sqrt{2}}(\lambda_1 \pm i\lambda_2), \\ \lambda_4^\pm &= \frac{1}{\sqrt{2}}(\lambda_4 \pm i\lambda_5), \\ \lambda_6^\pm &= \frac{1}{\sqrt{2}}(\lambda_6 \pm i\lambda_7). \end{aligned} \quad (33)$$

In the absence of pion condensate, $\phi_{ud} = 0$, the effective four-fermion interaction recovers the result obtained in the previous literature [20]. The scalar-pseudoscalar interaction $\mathcal{L}_{\text{KMT}}^{\text{sp}}$ is purely induced by the pion condensation.

Then the mesonic excitations can be studied by using the effective Lagrangian with only four-fermion interactions,

$$\mathcal{L}_{\text{eff}} = \bar{\psi}(i\gamma^\mu\partial_\mu - \hat{m}_0)\psi + \mathcal{L}_S + \mathcal{L}_{\text{KMT}}^{4f}. \quad (34)$$

For convenience, we rewrite the effective four-fermion interactions in a compact form,

$$\mathcal{L}_{\text{eff}} = \bar{\psi}(i\gamma^\mu \partial_\mu - \hat{m}_0)\psi + \Phi^\dagger \mathbf{G} \Phi, \quad (35)$$

where the bilinear field Φ is defined as

$$\Phi = \begin{pmatrix} \bar{\psi}\lambda_1^-\psi \\ \bar{\psi}\lambda_1^+\psi \\ \bar{\psi}\lambda_3^-\psi \\ \bar{\psi}\lambda_4^-\psi \\ \bar{\psi}\lambda_4^+\psi \\ \bar{\psi}\lambda_6^-\psi \\ \bar{\psi}\lambda_6^+\psi \\ \bar{\psi}\lambda_0^-\psi \\ \bar{\psi}\lambda_8^-\psi \\ \bar{\psi}i\gamma_5\lambda_1^-\psi \\ \bar{\psi}i\gamma_5\lambda_1^+\psi \\ \bar{\psi}i\gamma_5\lambda_3^-\psi \\ \bar{\psi}i\gamma_5\lambda_4^-\psi \\ \bar{\psi}i\gamma_5\lambda_4^+\psi \\ \bar{\psi}i\gamma_5\lambda_6^-\psi \\ \bar{\psi}i\gamma_5\lambda_6^+\psi \\ \bar{\psi}i\gamma_5\lambda_0^-\psi \\ \bar{\psi}i\gamma_5\lambda_8^-\psi \end{pmatrix} \quad (36)$$

and the effective coupling matrix \mathbf{G} takes the block form

$$\mathbf{G} = \begin{pmatrix} G_{11} & 0 & 0 & 0 & 0 & 0 & G_{17} \\ 0 & G_{22} & 0 & 0 & 0 & 0 & 0 \\ 0 & 0 & G_{33} & 0 & 0 & G_{36} & 0 \\ 0 & 0 & 0 & G_{44} & 0 & 0 & 0 \\ 0 & 0 & 0 & 0 & G_{55} & 0 & 0 \\ 0 & 0 & G_{63} & 0 & 0 & G_{66} & 0 \\ G_{71} & 0 & 0 & 0 & 0 & 0 & G_{77} \end{pmatrix}. \quad (37)$$

The nonvanishing blocks of \mathbf{G} are given by

$$\begin{aligned} G_{11} &= \left(G + \frac{K}{2}\sigma_s\right)I_2, \\ G_{22} &= G + \frac{K}{2}\sigma_s, \\ G_{33} &= \left(G + \frac{K}{2}\sigma_l\right)I_4, \\ G_{44} &= GI_4 + K \begin{pmatrix} A & \phi_{ud}B^T \\ \phi_{ud}B & -\frac{1}{2}\sigma_s I_2 \end{pmatrix}, \\ G_{55} &= G - \frac{K}{2}\sigma_s, \\ G_{66} &= \left(G - \frac{K}{2}\sigma_l\right)I_4, \\ G_{77} &= GI_2 - KA, \\ G_{17} &= G_{71}^T = K\phi_{ud}B, \\ G_{36} &= G_{63}^T = K\phi_{ud}C, \end{aligned} \quad (38)$$

where I_n is the $n \times n$ identity matrix, and the matrices $A, B,$

and C are defined as

$$\begin{aligned} A &= \begin{pmatrix} -\frac{1}{3}(2\sigma_l + \sigma_s) & \frac{\sqrt{2}}{6}(\sigma_l - \sigma_s) \\ \frac{\sqrt{2}}{6}(\sigma_l - \sigma_s) & \frac{1}{6}(4\sigma_l - \sigma_s) \end{pmatrix}, \\ B &= \frac{\sqrt{3}}{12} \begin{pmatrix} -1 & \sqrt{2} \\ -1 & \sqrt{2} \end{pmatrix}, \\ C &= \frac{1}{4} \begin{pmatrix} 0 & 0 & 1 & 0 \\ 0 & 0 & 0 & 1 \\ 1 & 0 & 0 & 0 \\ 0 & 1 & 0 & 0 \end{pmatrix}. \end{aligned} \quad (39)$$

Using the compact form of the effective four-fermion interaction, the meson propagator $\mathbf{D}(q)$ in the random-phase approximation can be expressed as

$$\mathbf{D}(q) = \frac{2\mathbf{G}}{\mathbf{1} - 2\mathbf{G}\mathbf{\Pi}(q)}, \quad (40)$$

where $q = (i\nu_n, \mathbf{q})$ with $\nu_n = 2\pi nT$ being the boson Matsubara frequency, and $\mathbf{\Pi}(q)$ is the polarization matrix given by

$$\mathbf{\Pi}_{mn}(q) = \int \frac{d^4k}{(2\pi)^4} \text{Tr} [\Gamma_m S(k+q) \Gamma_n^* S(k)] \quad (41)$$

with the mesonic vertex Γ_m defined as

$$\Gamma_m = \begin{cases} \lambda_1^- & m = a^+ \\ \lambda_1^+ & m = a^- \\ \lambda_3 & m = a_0 \\ \lambda_4^- & m = \kappa^+ \\ \lambda_4^+ & m = \kappa^- \\ \lambda_6^- & m = \kappa^0 \\ \lambda_6^+ & m = \bar{\kappa}^0 \\ \lambda_0 & m = \sigma_0 \\ \lambda_8 & m = \sigma_8 \\ i\gamma_5\lambda_1^- & m = \pi^+ \\ i\gamma_5\lambda_1^+ & m = \pi^- \\ i\gamma_5\lambda_3 & m = \pi_0 \\ i\gamma_5\lambda_4^- & m = K^+ \\ i\gamma_5\lambda_4^+ & m = K^- \\ i\gamma_5\lambda_6^- & m = K^0 \\ i\gamma_5\lambda_6^+ & m = \bar{K}^0 \\ i\gamma_5\lambda_0 & m = \eta_0 \\ i\gamma_5\lambda_8 & m = \eta_8 \end{cases} \quad (42)$$

After the analytical continuation $i\nu_n \rightarrow \omega + i0^+$, the meson masses are determined by the poles of the meson propagator $\mathbf{D}(\omega, \mathbf{q})$ at vanishing momentum \mathbf{q} , i.e.,

$$\det[\mathbf{1} - 2\mathbf{G}\mathbf{\Pi}(\omega = M_m, \mathbf{q} = 0)] = 0. \quad (43)$$

In the presence of pion condensate ϕ_{ud} , there arise some off-diagonal elements in the matrices \mathbf{G} and $\mathbf{\Pi}$ that do not appear for $\phi_{ud} = 0$. We define a matrix $\mathbf{M} \equiv \mathbf{1} - 2\mathbf{G}\mathbf{\Pi}$ and denote its elements as $M(i, j) = \mathbf{M}_{ij}$. After some matrix algebra, we find that the determinant of \mathbf{M} can be divided into some blocks,

$$\det \mathbf{M} = C_1 C_2 C_3 C_4 C_5 C_6 C_7 C_8, \quad (44)$$

where C_i are given by

$$\begin{aligned}
C_1 &= \det \begin{pmatrix} M(8,8) & M(8,9) & M(8,10) & M(8,11) \\ M(9,8) & M(9,9) & M(9,10) & M(9,11) \\ M(10,8) & M(10,9) & M(10,10) & M(10,11) \\ M(11,8) & M(11,9) & M(11,10) & M(11,11) \end{pmatrix}, \\
C_2 &= \det \begin{pmatrix} M(17,17) & M(17,18) & M(17,1) & M(17,2) \\ M(18,17) & M(18,18) & M(18,1) & M(18,2) \\ M(1,17) & M(1,18) & M(1,1) & M(1,2) \\ M(2,17) & M(2,18) & M(2,1) & M(2,2) \end{pmatrix}, \\
C_3 &= \det \begin{pmatrix} M(13,13) & M(13,6) \\ M(6,13) & M(6,6) \end{pmatrix}, \\
C_4 &= \det \begin{pmatrix} M(15,15) & M(15,4) \\ M(4,15) & M(4,4) \end{pmatrix}, \\
C_5 &= \det \begin{pmatrix} M(16,16) & M(16,5) \\ M(5,16) & M(5,5) \end{pmatrix}, \\
C_6 &= \det \begin{pmatrix} M(14,14) & M(14,7) \\ M(7,14) & M(7,7) \end{pmatrix}, \\
C_7 &= M(3,3), \\
C_8 &= M(12,12).
\end{aligned} \tag{45}$$

Other matrix elements of \mathbf{M} that do not appear above vanish automatically.

In the absence of pion condensate ϕ_{ud} , the nonvanishing off-diagonal elements are $M(8,9) = M(9,8)$ and $M(17,18) = M(18,17)$, which correspond to the $\sigma_0 - \sigma_8$ mixing and $\eta_0 - \eta_8$ mixing, respectively. At zero temperature and density, we recover the meson spectroscopy of three-flavor QCD. The $\eta_0 - \eta_8$ mixing and $\sigma_0 - \sigma_8$ mixing lead to the real mesonic excitations, the pseudoscalar η, η' mesons and scalar σ, f_0 mesons, respectively.

In the presence of pion condensate $\phi_{ud} \neq 0$, all the off-diagonal elements shown in Eq. (45) are nonzero. Therefore, the pion condensation generally leads to the mixing between the scalar and pseudoscalar mesons. First, from the expressions of C_7 and C_8 , we observe that the π_0 and a_0 are the eigenmodes of the mesonic excitations even in the presence of pion condensation. For other mesonic excitations, we have scalar-pseudoscalar mixing. In detail, the 4×4 matrix C_1 corresponds to the mixing between the scalar $\sigma_0 - \sigma_8$ sector and the pseudoscalar $\pi^+ - \pi^-$ sector. C_2 corresponds to the mixing between the scalar $a^+ - a^-$ sector and the pseudoscalar $\eta_0 - \eta_8$ sector. The 2×2 matrices C_3, C_4, C_5 , and C_6 describe the $K^+ - \kappa^0, K^0 - \kappa^+, \bar{K}^0 - \kappa^-, \text{ and } K^- - \bar{\kappa}^0$ mixing, respectively. Since we consider the case of zero strangeness chemical potential $\mu_S = 0$, we have

$$C_3 = C_5, \quad C_4 = C_6. \tag{46}$$

Therefore, the mesonic excitations from $K^+ - \kappa^0$ and $\bar{K}^0 - \kappa^-$ mixing are degenerate, and the excitations from $K^0 - \kappa^+$ and $K^- - \bar{\kappa}^0$ mixing are also degenerate.

Now we turn to our numerical results. We focus on the following three cases: (A) $\mu_I = 0, T \neq 0$, (B) $\mu_I \neq 0, T = 0$, and (C) $\mu_I \neq 0, T \neq 0$. Here we emphasize two points before we present the numerical results: (1) In the superfluid phase with $\phi_{ud} \neq 0$, only the π_0 and a_0 mesons carry the same quantum

numbers as those in the vacuum; other mesonic excitations are generally mixtures of scalar and pseudoscalar contents. Therefore, we may name the mesonic excitations in the superfluid phase by using the mesons in the normal phase according to the fact that their masses are generally continuous at the superfluid phase transition. (2) Some mesonic excitations have nonzero decay width at high temperature and chemical potential. Here we focus on their real part masses.

A. $\mu_I = 0, T \neq 0$

At finite temperature and vanishing isospin chemical potential, pion condensation does not occur. Therefore, we have only the $\eta_0 - \eta_8$ mixing and $\sigma_0 - \sigma_8$ mixing induced by the $U_A(1)$ anomaly. In this paper, we consider the case that the $U_A(1)$ strength K does not depend on the temperature. While the mixing persists to exist at finite temperature, the meson masses and the mixing angles change with increasing temperature.

In Fig. 9, we show the meson masses with increasing temperature T at $\mu_I = 0$. Due to vanishing chemical potentials, the masses of π^+, π^- and π_0 are degenerate (denoted by π), the masses of K^+, K^-, K^0 and \bar{K}^0 are degenerate (denoted by K), and the masses of $\kappa^+, \kappa^-, \kappa^0$ and $\bar{\kappa}^0$ are degenerate (denoted by κ). Our results are consistent with those reported in the previous studies [26, 27]. From the results of the chiral condensates shown in Fig. 1, we observe that the $SU_A(2)$ chiral symmetry for light quarks becomes approximately restored at high temperature. This fact is also reflected in the meson mass spectra. At high enough temperature, we find that the masses of the $SU(2)$ chiral partners (π - σ , K - κ , and a - η) become approximately degenerate.

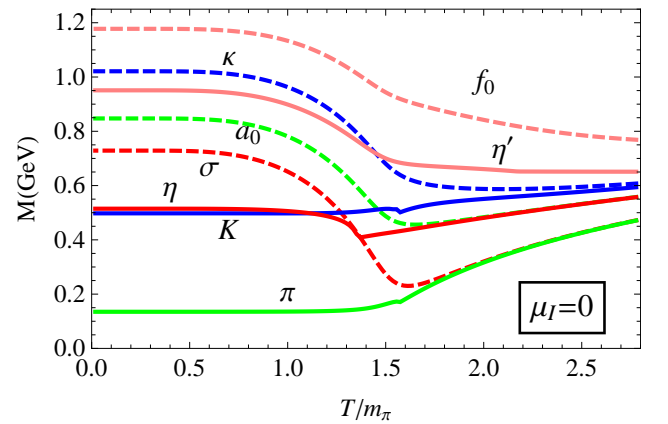


FIG. 9. (color-online). The meson masses as functions of temperature T at zero isospin chemical potential.

B. $\mu_I \neq 0, T = 0$

At zero temperature, the system undergoes a quantum phase transition from the vacuum to the pion condensed phase at

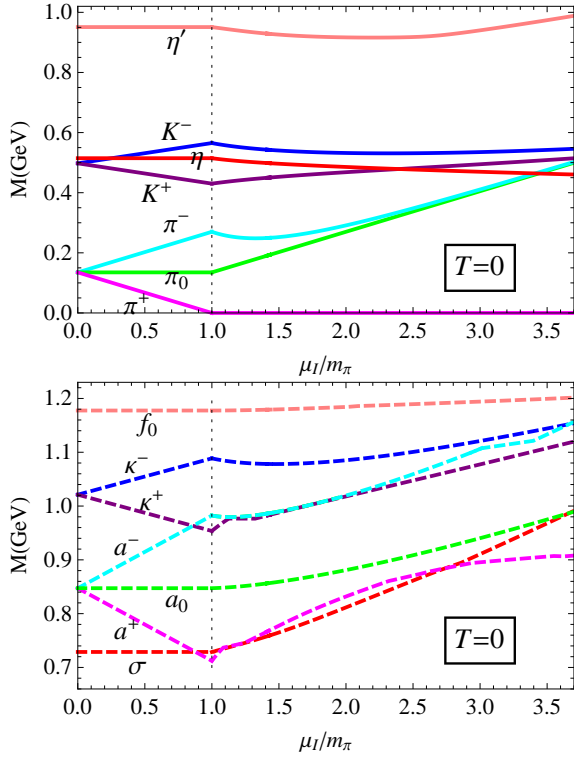


FIG. 10. (color-online). The meson mass spectra at finite isospin chemical potential and zero temperature.

$\mu_I = m_\pi$. It is interesting to study the behavior mesonic excitations across this phase transition. Since we consider vanishing strangeness chemical potential μ_S , the mesonic excitations from $K^+ - \kappa^0$ and $\bar{K}^0 - \kappa^-$ mixing are degenerate and the excitations from $K^0 - \kappa^+$ and $K^- - \bar{\kappa}^0$ mixing are also degenerate. Therefore, in the following we only show the masses of K^\pm and κ^\pm mesons. The numerical results for the meson masses as functions of the isospin chemical potential are shown in Fig. 10.

In the regime $\mu_I < m_\pi$, pion condensation does not occur and we have $\phi_{ud} = 0$. At zero temperature, the mesonic excitations are the same as those in the vacuum, except for the fact that the pole masses are shifted by the isospin chemical potential. For a meson that carries an isospin quantum number I , its mass at finite isospin chemical potential reads

$$M_I = M_v - I\mu_I, \quad \mu_I < m_\pi, \quad (47)$$

where M_v is its mass in the vacuum. This result can be understood by the fact that its energy-momentum dispersion at finite isospin chemical potential reads $\omega(\mathbf{q}) = \sqrt{\mathbf{q}^2 + M_v^2} - I\mu_I$ and its mass is defined as the pole $M_I = \omega(\mathbf{0})$ at zero momentum. We note that since the pions are the lightest meson in the meson spectra, the π^+ mass first drops down to zero at $\mu_I = m_\pi$. This is consistent with the fact that the charged pions rather than other mesons start to condense at $\mu_I = m_\pi$.

In the superfluid phase $\mu_I > m_\pi$, there exists not only the mixing induced by the $U_A(1)$ anomaly but also the scalar-pseudoscalar mixing induced by the nonvanishing pion condensate $\phi_{ud} \neq 0$. The masses of the mesonic excitations in the

superfluid phase should be determined by solving the equations,

$$C_i(\omega = M_m, \mathbf{q} = 0) = 0, \quad i = 1, 2, \dots, 8. \quad (48)$$

First, at finite isospin chemical potential $\mu_I \neq 0$, the flavor symmetry for the light quarks, $SU_L(2) \times SU_R(2)$, is explicitly broken down to $U_L(1) \times U_R(1) \equiv U_I(1) \times U_{IA}(1)$ with the generator being the third component of the isospin (I_3). We note that the residual $U_I(1)$ symmetry is exact even for nonvanishing current quark mass m_q . The $U_I(1)$ symmetry is spontaneously broken by the nonzero pion condensate $\phi_{ud} \neq 0$, leading to Bose-Einstein condensation of pions. Therefore, we expect that a massless mesonic excitation appears in the meson spectra, corresponding to the Goldstone mode in a superfluid. Using the gap equations for the condensates σ_q , σ_s , and ϕ_{ud} , we find analytically that

$$C_1(\omega = 0, \mathbf{q} = 0) = 0. \quad (49)$$

Therefore, our treatment of the condensates and the collective excitations self-consistently results in a massless mode, i.e., the Goldstone mode. The masses of the other mesonic excitations can only be solved numerically, except for the π_0 mass. For the π_0 meson, we have analytically $M_{\pi_0} = \mu_I$, which is the same as that predicted by the two-flavor models [6, 29].

The numerical results for the mass spectra are shown in Fig. 10. We only denote the names of the mesonic excitations in the normal phase $\mu_I < m_\pi$, where the mesons carry the same quantum numbers as in the vacuum. In the superfluid phase $\mu_I > m_\pi$, only the π_0 and a_0 modes carry their vacuum quantum numbers. For other mesonic excitations, they generally contain both scalar and pseudoscalar contents. However, we still name the mesonic excitations in the superfluid phase according to the fact that their masses are continued with the mesons in the normal phase at the phase transition $\mu_I = m_\pi$. At finite isospin chemical potential, the $SU_A(2)$ chiral symmetry for the light quarks is explicitly broken down to $U_{IA}(1)$. Since the chiral condensates for light quarks become very small at large isospin chemical potential, we may expect approximate restoration of the chiral symmetry in the superfluid phase. Actually, at large isospin chemical potential (e.g., $\mu_I = 3m_\pi$), we find that the content of the “ π^- meson” is almost that of the σ meson. Therefore, the degeneracy of the masses of the π_0 and π^- meson reflects the approximate restoration of the chiral symmetry.

$$C. \quad \mu_I \neq 0, T \neq 0$$

Finally, we discuss the general case of nonzero temperature and isospin chemical potential. First, let us fix the isospin chemical potential $\mu_I = 250\text{MeV}$ and study the mesonic excitations across the temperature-induced superfluid phase transition. The finite-temperature behavior of the chiral and pion condensates is shown in Fig. 4, which indicates a superfluid phase transition at $T = T_c = 187.2\text{MeV}$. The finite-temperature behavior of the meson masses for fixed $\mu_I = 250\text{MeV}$ is shown in Fig. 11.

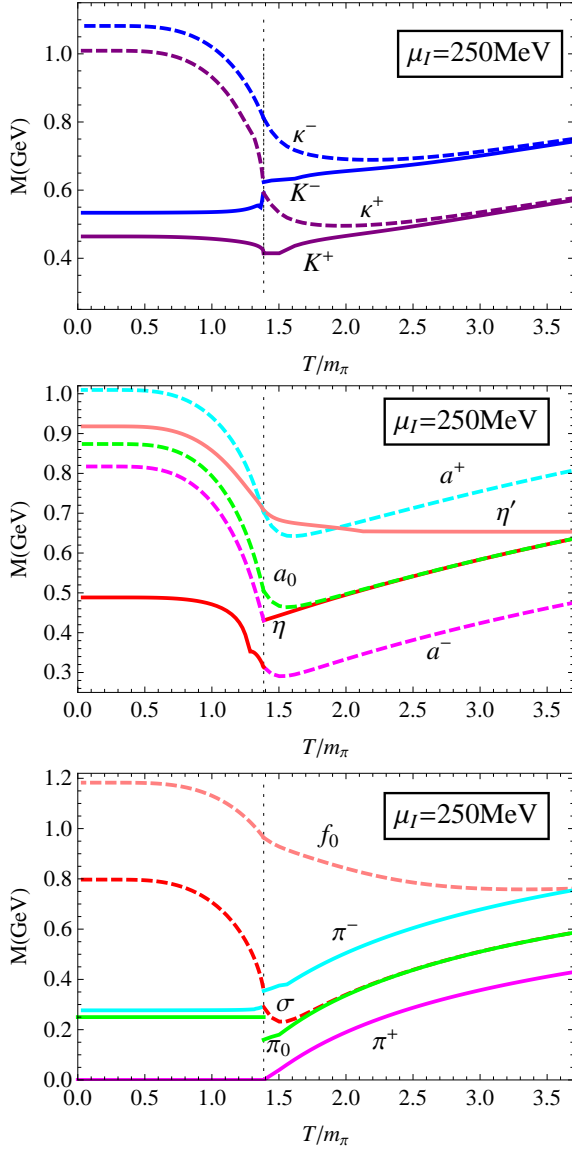


FIG. 11. (color-online). The meson masses as functions of the temperature T at fixed isospin chemical potential $\mu_I = 250\text{MeV}$. The thin dashed lines denote the superfluid phase transition at $T = T_c = 187.2\text{MeV}$.

In the superfluid phase $T < T_c$, the mesonic excitations except for π_0 and a_0 contain both scalar and pseudoscalar contents. We name the excitations according to the fact that their masses are continuous in the regime $T < T_c$, and we have named the mesonic excitations at $T = 0$ in Fig. 10. Above the critical temperature T_c , the pion condensate ϕ_{ud} vanishes and all mesonic excitations can be characterized by their quantum numbers. In Fig. 11, we observe that some meson masses are discontinuous across the superfluid phase transition. At high temperature, since the light quark chiral condensate becomes very small, we expect that the residual U_{IA} chiral symmetry gets restored. Actually, we find that the masses of the $U(1)$ chiral partners ($K^+ - \kappa^+$, $K^- - \kappa^-$, $\pi_0 - \sigma$, and $a_0 - \eta$) become approximately degenerate.

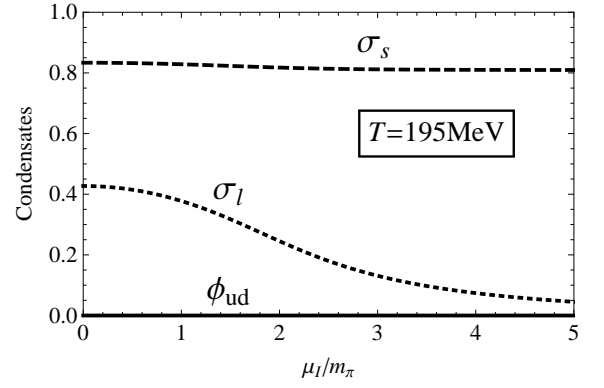


FIG. 12. The chiral and pion condensates as functions of the isospin chemical potential μ_I at fixed temperature $T = 195\text{MeV}$.

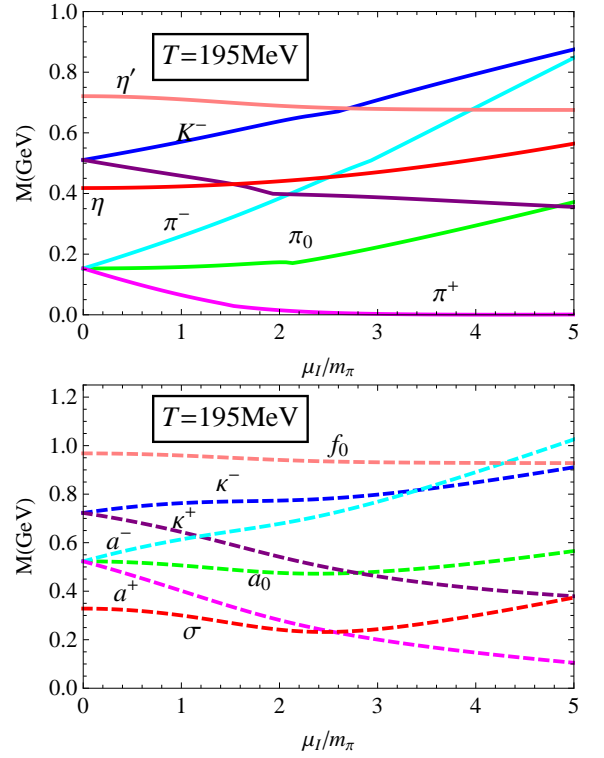


FIG. 13. (color-online). The meson masses as functions of the isospin chemical potential μ_I at fixed temperature $T = 195\text{MeV}$.

Next we fix the temperature $T = 195\text{MeV}$ and study the isospin splitting effect on the mesonic excitations. The behavior of the chiral and pion condensates at $T = 195\text{MeV}$ is shown in Fig. 12. The pion condensate ϕ_{ud} always vanishes and the light quark chiral condensate σ_q becomes small at large isospin chemical potential. Since the pion condensate vanishes, all mesonic excitations can be characterized by their quantum numbers. The meson mass spectra are shown in Fig. 13. We find clearly that the mass splitting of the isospin partners ($K^+ - K^-$, $\kappa^+ - \kappa^-$, $\pi^+ - \pi^-$ and $a^+ - a^-$) becomes larger and larger with increasing isospin chemical potential.

IV. TOPOLOGICAL SUSCEPTIBILITY AT FINITE ISOSPIN DENSITY

The topological susceptibility χ is a fundamental correlation function in QCD and is the key to understanding much of the distinctive dynamics in the $U_A(1)$ channel. In this section we calculate the topological susceptibility χ at finite isospin chemical potential μ_I within the framework of the three-flavor NJL model. The general expression of χ to the leading order in the $1/N_c$ expansion at finite temperature and vanishing chemical potentials for the NJL model has been derived by Fukushima *et al.* [23]. On the other hand, the finite-temperature behavior of the topological susceptibility can be determined by lattice simulations of QCD at $T \neq 0$ [24]. Therefore, the temperature dependence of the $U_A(1)$ anomaly strength K in the NJL model can be determined by using the lattice data. A vanishingly small K at high temperature can be regarded as the effective restoration of the $U_A(1)$ symmetry.

Since there are no lattice data for the topological susceptibility at finite μ_I , in this section we study the behavior of χ at finite μ_I , by treating the $U_A(1)$ anomaly strength K as a constant. The μ_I dependence of the $U_A(1)$ anomaly strength K may be determined if lattice data for χ at finite μ_I are available in the future. In the following we first derive a general expression of χ to the leading order in the $1/N_c$ expansion at finite isospin chemical potential and temperature, where the pion condensate ϕ_{ud} can be nonzero. To this end, we first show the definition of χ and therefore start with the QCD Lagrangian density,

$$\mathcal{L}_{\text{QCD}} = -\frac{1}{4}F_{\mu\nu}^a F^{a\mu\nu} + \bar{\psi}(i\gamma_\mu D^\mu - \hat{m}_0)\psi + \theta Q \quad (50)$$

where $F_{\mu\nu}^a$ represents the gluon field strength tensor, $D_\mu = \partial_\mu + igA_\mu$ is the covariant derivative with A_μ being the gluon field and g the QCD coupling constant, θ is the QCD vacuum angle, and Q is the topological charge density. The topological charge density Q is given by

$$Q(x) = \frac{g^2}{32\pi^2} F_{\mu\nu}^a \tilde{F}^{a\mu\nu}. \quad (51)$$

The topological susceptibility χ can be defined as a second-

order derivative of the vacuum energy density ε with respect to θ at $\theta = 0$,

$$\chi = \left. \frac{\partial^2 \varepsilon}{\partial \theta^2} \right|_{\theta=0} = \int d^4x \langle 0 | T Q(x) Q(0) | 0 \rangle_{\text{connected}}, \quad (52)$$

where T denotes the time-ordering operator, and the subscript “connected” means to pick out the diagrammatically connected contributions. On the other hand, χ can also be regarded as the zero frequency mode of the Fourier transform of the correlation function $\langle T Q(x) Q(0) \rangle$,

$$\chi = \lim_{k \rightarrow 0} \int d^4x e^{-ik \cdot x} \langle T Q(x) Q(0) \rangle. \quad (53)$$

In order to calculate χ in the NJL model, we need to find a correspondent to $Q(x)$ in the model. In QCD the axial current $J_5^\mu = \bar{\psi} \gamma^5 \gamma^\mu \psi$ is not conserved due to the $U_A(1)$ anomaly induced by the instanton effect. This fact can be expressed as

$$\partial_\mu J_5^\mu(x) = 2N_f Q(x) + 2i\bar{\psi} m \gamma_5 \psi. \quad (54)$$

On the other hand, in the NJL model, the $U_A(1)$ anomaly is caused by the KMT term. We find [23]

$$\partial_\mu J_5^\mu = 4N_f K \text{Im} \det \Phi + 2i\bar{\psi} m \gamma_5 \psi, \quad (55)$$

where $\Phi_{ij} = \bar{\psi}_i(1 - \gamma_5)\psi_j$ with i, j being the flavor indices. Comparing the expressions (54) and (55), we find that the topological charge density in the NJL model can be defined as

$$Q(x) = 2K \text{Im} \det \Phi = -iK [\det \Phi - (\det \Phi)^*]. \quad (56)$$

Having obtained the expression of the topological charge density $Q(x)$ in the NJL model, we can go on to calculate the topological susceptibility χ according to the definition (52). Using the identities

$$\begin{aligned} \det \Phi &= \epsilon^{ijk} (\bar{\psi}_u \Gamma_- \psi_i) (\bar{\psi}_d \Gamma_- \psi_j) (\bar{\psi}_s \Gamma_- \psi_k), \\ (\det \Phi)^* &= \epsilon^{lmn} (\bar{\psi}_u \Gamma_+ \psi_l) (\bar{\psi}_d \Gamma_+ \psi_m) (\bar{\psi}_s \Gamma_+ \psi_n), \end{aligned} \quad (57)$$

where $\Gamma_\pm = 1 \pm \gamma_5$ and the summation over the flavor indices (i, j, k, l, m, n) is implicit, we can express the topological susceptibility χ as [23]

$$\begin{aligned} \chi &= \int d^4x \langle 0 | T Q(x) Q(0) | 0 \rangle_{\text{connected}} \\ &= -K^2 \int d^4x \epsilon^{ijk} \epsilon^{lmn} \langle 0 | T \{ (\bar{\psi}_u \Gamma_- \psi_i) (\bar{\psi}_d \Gamma_- \psi_j) (\bar{\psi}_s \Gamma_- \psi_k)(x) (\bar{\psi}_u \Gamma_+ \psi_l) (\bar{\psi}_d \Gamma_+ \psi_m) (\bar{\psi}_s \Gamma_+ \psi_n)(0) \\ &\quad - (\bar{\psi}_u \Gamma_- \psi_i) (\bar{\psi}_d \Gamma_- \psi_j) (\bar{\psi}_s \Gamma_- \psi_k)(x) (\bar{\psi}_u \Gamma_+ \psi_l) (\bar{\psi}_d \Gamma_+ \psi_m) (\bar{\psi}_s \Gamma_+ \psi_n)(0) \\ &\quad - (\bar{\psi}_u \Gamma_+ \psi_i) (\bar{\psi}_d \Gamma_+ \psi_j) (\bar{\psi}_s \Gamma_+ \psi_k)(x) (\bar{\psi}_u \Gamma_- \psi_l) (\bar{\psi}_d \Gamma_- \psi_m) (\bar{\psi}_s \Gamma_- \psi_n)(0) \\ &\quad + (\bar{\psi}_u \Gamma_+ \psi_i) (\bar{\psi}_d \Gamma_+ \psi_j) (\bar{\psi}_s \Gamma_+ \psi_k)(x) (\bar{\psi}_u \Gamma_- \psi_l) (\bar{\psi}_d \Gamma_- \psi_m) (\bar{\psi}_s \Gamma_- \psi_n)(0) \} | 0 \rangle_{\text{connected}}. \end{aligned} \quad (58)$$

Next we need to evaluate the above four matrix elements. Following Wick's theorem, we take full contraction in terms of the quark propagator $\mathcal{S}(x, x')$ which has been constructed

in Eq. (20) with the condensates determined by the self-consistent gap Eqs. (24).

To be self-consistent, we consider only the leading-order

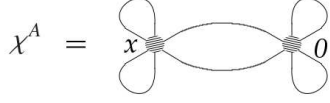


FIG. 14. The simplest leading-order contribution to the topological susceptibility in the $1/N_c$ expansion. The gray circle denotes the $U_A(1)$ anomaly coupling K .

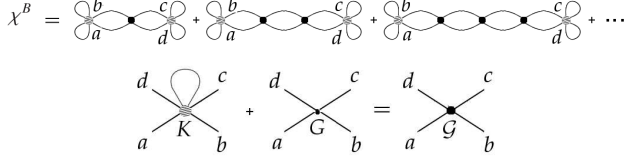


FIG. 15. Other leading-order contributions (ring diagrams) to the topological susceptibility.

contributions in the $1/N_c$ expansion. The simplest leading-order contribution $\chi^A \sim O(N_c^5)$ is shown in Fig. 14. In the presence of pion condensate ϕ_{ud} , the quark propagator $S(x, x')$ is not diagonal in the flavor space. This brings many more contributions than the case of $\phi_{ud} = 0$. To evaluate χ^A , we just need to replace the topological charge density $Q(x)$ by its mean-field approximation

$$Q_{\text{mf}}(x) \simeq \left(\frac{1}{2\sqrt{6}} |\phi_{ud}|^2 + \frac{4}{\sqrt{6}} \sigma_l \sigma_s + \frac{2}{\sqrt{6}} \sigma_l^2 \right) K(\bar{\psi} \lambda_0 i \gamma_5 \psi) + \left(-\frac{1}{2\sqrt{3}} |\phi_{ud}|^2 + \frac{2}{\sqrt{3}} \sigma_l \sigma_s - \frac{2}{\sqrt{3}} \sigma_l^2 \right) K(\bar{\psi} \lambda_8 i \gamma_5 \psi) - \frac{1}{\sqrt{2}} \phi_{ud}^* K \sigma_s (\bar{\psi} \lambda_1^+ \psi) - \frac{1}{\sqrt{2}} \phi_{ud} K \sigma_s (\bar{\psi} \lambda_1^- \psi). \quad (59)$$

Then the contribution χ^A can be expressed in a compact form,

$$\chi^A = 4K^2 P^T \Pi P, \quad (60)$$

where the matrices P and Π are given by

$$P = \begin{pmatrix} \frac{-1}{4\sqrt{6}} |\phi_{ud}|^2 - \frac{2}{\sqrt{6}} \sigma_l \sigma_s - \frac{1}{\sqrt{6}} \sigma_l^2 \\ \frac{1}{4\sqrt{3}} |\phi_{ud}|^2 - \frac{2}{\sqrt{3}} \sigma_l \sigma_s + \frac{1}{\sqrt{3}} \sigma_l^2 \\ \frac{1}{2\sqrt{2}} \phi_{ud}^* \sigma_s \\ \frac{1}{2\sqrt{2}} \phi_{ud} \sigma_s \end{pmatrix} \quad (61)$$

and

$$\Pi = \begin{pmatrix} \Pi_{\eta_0 \eta_0} & \Pi_{\eta_0 \eta_8} & \Pi_{\eta_0 a^+} & \Pi_{\eta_0 a^-} \\ \Pi_{\eta_8 \eta_0} & \Pi_{\eta_8 \eta_8} & \Pi_{\eta_8 a^+} & \Pi_{\eta_8 a^-} \\ \Pi_{a^+ \eta_0} & \Pi_{a^+ \eta_8} & \Pi_{a^+ a^+} & \Pi_{a^+ a^-} \\ \Pi_{a^- \eta_0} & \Pi_{a^- \eta_8} & \Pi_{a^- a^+} & \Pi_{a^- a^-} \end{pmatrix}. \quad (62)$$

Note that the matrix Π is actually the matrix in the determinant C_2 , but evaluated at $(\omega, \mathbf{q}) = (0, \mathbf{0})$.

Other contributions to χ that are of the same order in $1/N_c$ expansion as χ^A are shown in Fig. 15. They are regarded as the ring diagrams, and we have to include all these ring diagrams for consistency of the $1/N_c$ expansion. They are of

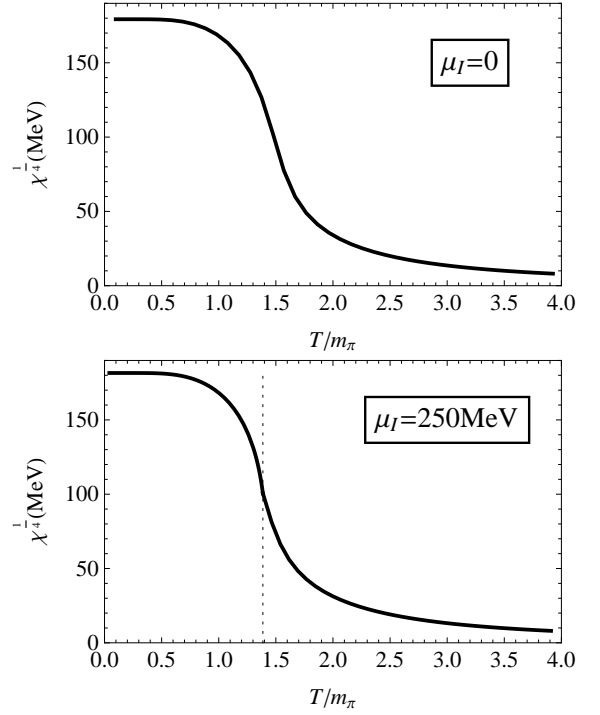


FIG. 16. The topological susceptibility χ (we show $\chi^{1/4}$) as a function of temperature T for $\mu_I = 0$ and $\mu_I = 250 \text{ MeV}$. The thin dashed line denotes the superfluid phase transition.

the same order as Fig. 14. To show this, we notice that while each four-point vertex is of order $O(N_c^{-1})$, it is compensated by a factor N_c coming from its neighboring loop. The sum of these ring diagrams with the one-loop diagram included can be physically interpreted as the propagations of some certain mesonic modes. In the absence of the pion condensate, it can be interpreted as the propagations of η_0 and η_8 mesons as well as their mixing. However, for $\phi_{ud} \neq 0$, we will see that the propagations of a^\pm mesons as well as their mixing with η_0 and η_8 mesons are involved. Note that the energy and momentum of the propagating mesonic modes are zero; $(\omega, \mathbf{q}) = (0, \mathbf{0})$, which just reflects the fact that χ is the zero frequency mode of the Fourier transform of $\langle TQ(x)Q(0) \rangle$. Summing all these ring diagrams, we find that the contribution χ^B can be expressed as

$$\chi^B = 4K^2 P^T \Pi \frac{2\mathcal{G}}{1 - 2\mathcal{G}\Pi} \Pi P, \quad (63)$$

where the effective coupling matrix \mathcal{G} is given by

$$\mathcal{G} = GI_4 + K \begin{pmatrix} -A & \phi_{ud} B^T \\ \phi_{ud} B & \frac{1}{2} \sigma_s I_2 \end{pmatrix}. \quad (64)$$

Here the matrices A and B have been defined in (39).

The final result for the topological susceptibility reads

$$\chi = \chi^A + \chi^B = 4K^2 P^T \frac{\Pi}{1 - 2\mathcal{G}\Pi} P. \quad (65)$$

At vanishing isospin chemical potential, $\mu_I = 0$, by setting the pion condensate $\phi_{ud} = 0$, we find that the above result for χ recovers the one derived by Fukushima *et al.* [23].

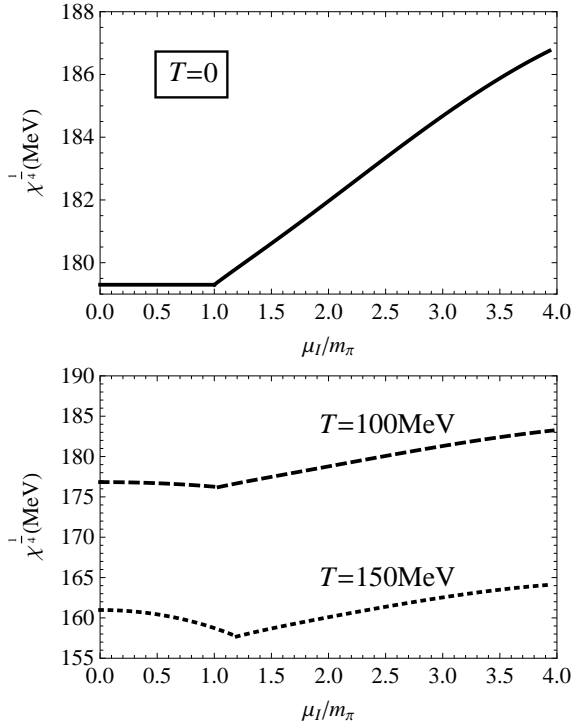


FIG. 17. The topological susceptibility χ (we show $\chi^{1/4}$) as a function of μ_I for $T = 0$ and $T \neq 0$.

Now we present the numerical results for the topological susceptibility χ at finite isospin chemical potential and at finite temperature. For our model parameter set, the topological susceptibility χ in the vacuum reads $\chi_0 = (179.3 \text{ MeV})^4$, consistent with the lattice data [24]. In Fig. 16, we show the finite-temperature behavior of χ at vanishing and at finite isospin chemical potentials. We find that the temperature effect leads to suppression of the topological susceptibility, both in the normal phase and in the pion superfluid phase. We may expect that the density effect would also reduce the topological susceptibility. The behavior of χ with increasing isospin chemical potential μ_I is shown in Fig. 17. However, we find that the isospin density effect is quite different from the temperature effect. At zero temperature, χ keeps its vacuum value in the regime $\mu_I < m_\pi$ and then starts to increase with increasing μ_I in the superfluid phase $\mu_I > m_\pi$, where a nonzero isospin density n_I is generated. At finite temperature, χ first decreases in the normal phase and reaches a minimum at the superfluid transition. In the superfluid phase, χ becomes again enhanced by the isospin chemical potential. However, the increase in the topological susceptibility is not large. At zero temperature, the quantity $\chi^{1/4}$ is increased by only about 8 MeV at $\mu_I = 4m_\pi$. The enhancement of the topological susceptibility at finite isospin density is similar to the behavior of the gluon condensate [30], which also gets enhanced by the

isospin density effect.

Finally, we point out that the numerical results presented above are obtained by treating the $U_A(1)$ anomaly K as a constant, which implies no effective restoration of the $U_A(1)$ symmetry. However, it is generally believed that the $U_A(1)$ symmetry becomes effectively restored at high density and therefore K is generally μ_I dependent. The behavior of χ observed above could be qualitatively reliable at small and even at moderate isospin density, since we expect the density dependence of K is slight there. At large enough isospin density, we expect K goes to zero and the $U_A(1)$ symmetry gets effectively restored. If the lattice data for χ at finite μ_I becomes available in the future, we can determine the μ_I dependence of K and therefore study the restoration of the $U_A(1)$ symmetry at finite density.

V. SUMMARY

In summary, we have studied the three-flavor Nambu–Jona-Lasinio model with $U_A(1)$ anomaly at finite isospin chemical potential. Similar to the two-flavor models, the three-flavor NJL model also predicts a quantum phase transition from the vacuum to the pion superfluid phase, which takes place exactly at $\mu_I = m_\pi$. However, due to the $U_A(1)$ anomaly, the strangeness degree of freedom couples to the light quark degrees of freedom, and the strange quark effective mass depends on the pion condensate. This coupling is absent if the $U_A(1)$ anomaly strength K is turned off. Numerically, we find that the strange quark condensate and the strange quark effective mass change very slightly in the pion superfluid phase, which verifies the validity of the two-flavor models. To study the mesonic excitations in the isospin dense medium, we have constructed the effective four-fermion interaction of the KMT term in the presence of pion condensation. We find that the pion condensation generally induces scalar-pseudoscalar interaction in the presence of $U_A(1)$ anomaly strength K . The propagator of the mesonic excitations is established within the framework of the random-phase approximation. The meson mass spectra are studied at finite isospin chemical potential and temperature. Finally, we have derived the general expression for the topological susceptibility χ at finite isospin chemical potential with nonvanishing pion condensate. We find that the topological susceptibility χ gets enhanced in the pion superfluid phase; that is, the isospin density effect leads to the enhancement of χ , in contrast to the finite temperature effect which generally reduces χ . Our model predictions may be tested by future lattice simulations of 2 + 1 flavor QCD at finite isospin density.

Acknowledgements: T. X. and P. Z. are supported by the NSFC under Grant No. 11079024 and the MOST under Grant No. 2013CB922000, and L. H. acknowledges the support from the Helmholtz International Center for FAIR within the framework of the LOEWE program launched by the state of Hesse.

-
- [1] F. Karsch, Lect. Notes Phys. **583**, 209(2002); S. Muroya, A. Nakamura, C. Nonaka and T. Takaishi, Prog. Theor. Phys. **110**, 615(2003).
- [2] J. B. Kogut, M. A. Stephanov and D. Toublan, Phys. Lett. **B464**, 183(1999); J. B. Kogut, M. A. Stephanov, D. Toublan, J. J. M. Verbaarschot and A. Zhitnitsky, Nucl. Phys. **B582**, 477(2000); K. Splittorff, D. T. Son and M. A. Stephanov, Phys. Rev. **D64**, 016003(2001); J. T. Lenaghan, F. Sannino and K. Splittorff, Phys. Rev. **D65**, 054002(2002); K. Splittorff, D. Toublan and J. J. M. Verbaarschot, Nucl. Phys. **B620**, 290(2002); K. Splittorff, D. Toublan and J. J. M. Verbaarschot, Nucl. Phys. **B639**, 524(2002); C. Ratti and W. Weise, Phys. Rev. **D70**, 054013(2004); T. Brauner, K. Fukushima and Y. Hidaka, Phys. Rev. **D80**, 074035(2009); J. O. Andersen and T. Brauner, Phys. Rev. **D81**, 096004(2010); T. Zhang, T. Brauner and D. H. Rischke, JHEP **1006**, 064(2010); N. Strodthoff, B.-J. Schaefer, and L. von Smekal, Phys. Rev. **D85**, 074007(2012); L. von Smekal, Nucl. Phys. Proc. Suppl. **228**, 179(2012).
- [3] S. Hands, I. Montvay, S. Morrison, M. Oevers, L. Scorzato and J. Skullerud, Eur. Phys. J. **C17**, 285(2000); S. Hands, I. Montvay, L. Scorzato and J. Skullerud, Eur. Phys. J. **C22**, 451(2001); J. B. Kogut, D. K. Sinclair, S. J. Hands and S. E. Morrison, Phys. Rev. **D64**, 094505(2001); J. B. Kogut, D. Toublan and D. K. Sinclair, Phys. Lett. **B514**, 77(2001); S. Hands, S. Kim and J. Skullerud, Eur. Phys. J. **C48**, 193(2006); S. Hands, S. Kim and J. Skullerud, Phys. Rev. **D81**, 091502(R)(2010); B. Alles, M. D'Elia, M. P. Lombardo, Nucl. Phys. **B752**, 124(2006).
- [4] D. T. Son and M. A. Stephanov, Phys. Rev. Lett. **86**, 592(2001); Phys. Atom. Nucl. **64**, 834(2001).
- [5] M. Loewe and C. Villavicencio, Phys. Rev. **D67**, 074034(2003); D. Toublan and J. B. Kogut, Phys. Lett. **B564**, 212(2003); M. Frank, M. Buballa and M. Oertel, Phys. Lett. **B562**, 221(2003); A. Barducci, R. Casalbuoni, G. Pettini and L. Ravagli, Phys. Rev. **D69**, 096004(2004); D. Ebert and K. G. Klimenko, Eur. Phys. J. **C46**, 771(2006); Z. Zhang and Y.-X. Liu, Phys. Rev. **C75**, 064910(2007); J. O. Andersen, Phys. Rev. **D75**, 065011(2007); S. Shu and J. Li, J. Phys. **G34**, 2727(2007); T. Herpay and P. Kovacs, Phys. Rev. **D78**, 116008(2008); J. Xiong, M. Jin and J. Li, J. Phys. **G36**, 125005(2009); J. O. Andersen and L. Kyllingstad, J. Phys. **G37**, 015003(2009); H. Abuki, R. Anglani, R. Gatto, M. Pellicoro, and M. Ruggieri, Phys. Rev. **D79**, 034032(2009); E. S. Fraga, L. F. Palhares, and C. Villavicencio, Phys. Rev. **D79**, 014021(2009); T. Sasaki, Y. Sakai, H. Kouno, and M. Yahiro, Phys. Rev. **D82**, 116004(2010); E. E. Svanes and J. O. Andersen, Nucl. Phys. **A857**, 16(2011); K. Kamikado, N. Strodthoff, L. von Smekal and J. Wambach, Phys. Lett. **B718**, 1044(2013); R. Stiele, E. S. Fraga, and J. Schaffner-Bielich, arXiv:1307.2851.
- [6] L. He and P. Zhuang, Phys. Lett. **B615**, 93(2005); L. He, M. Jin and P. Zhuang, Phys. Rev. **D71**, 116001(2005); Phys. Rev. **D74**, 036005(2006); C.-F. Mu, L. He, and Y.-X. Liu, Phys. Rev. **D82**, 056006(2010).
- [7] J. B. Kogut, D. K. Sinclair, Phys. Rev. **D66**, 034505(2002); Phys. Rev. **D66**, 014508(2002); Phys. Rev. **D70**, 094501(2004); P. Forcrand, M. A. Stephanov and U. Wenger, PoSLAT2007, 237(2007).
- [8] For a review of weakly interacting Bose condensate, see J. O. Andersen, Rev. Mod. Phys. **76**, 599(2004).
- [9] R. F. Sawyer, Phys. Rev. Lett. **29**, 382(1972).
- [10] D. J. Scalapino, Phys. Rev. Lett. **29**, 386(1972).
- [11] G. Baym, Phys. Rev. Lett. **30**, 1340(1973).
- [12] D. K. Campbell, R. F. Dashen and J. T. Manassah, Phys. Rev. **D12**, 979(1975); *ibid* **D12**, 1010(1975).
- [13] D. T. Son, Phys. Rev. **D59**, 094019(1999); T. Schäfer and F. Wilczek, Phys. Rev. **D60**, 114033(1999); D. Pisarski and D. H. Rischke, Phys. Rev. **D61**, 074017(2000); T. Kanazawa, T. Wettig and N. Yamamoto, JHEP **0908**, 003(2009).
- [14] D. M. Eagles, Phys. Rev. **186**, 456(1969).
- [15] A. J. Leggett, in *Modern Trends in the Theory of Condensed Matter*, edited by A. Pekalski and R. Przystawa, Springer-Verlag, Berlin(1980).
- [16] P. Nozieres and S. Schmitt-Rink, J. Low Temp. Phys. **59**, 195(1985); C. A. R. Sa de Melo, Mohit Randeria, and Jan R. Engelbrecht, Phys. Rev. Lett. **71**, 3202(1993); Q. Chen, J. Stajic, S. Tan, and K. Levin, Phys. Rep. **412**, 1(2005); S. Giorgini, L. P. Pitaevskii, and S. Stringari, Rev. Mod. Phys. **80**, 1215(2008).
- [17] Y. Nishida and H. Abuki, Phys. Rev. **D72**, 096004(2005); H. Abuki, Nucl. Phys. **A791**, 117(2007); L. He and P. Zhuang, Phys. Rev. **D75**, 096003(2007); Phys. Rev. **D76**, 056003(2007); J. Deng, A. Schmitt and Q. Wang, Phys. Rev. **D76**, 034013(2007); J. Deng, J.-C. Wang and Q. Wang, Phys. Rev. **D78**, 034014(2008); T. Brauner, Phys. Rev. **D77**, 096006(2008); H. Abuki and T. Brauner, Phys. Rev. **D78**, 125010(2008); D. Blaschke and D. Zablocki, Phys. Part. Nucl. **39**, 1010(2008); B. Chatterjee, H. Mishra, and A. Mishra, Phys. Rev. **D79**, 014003(2009); H. Guo, C.-C. Chien, and Y. He, Nucl. Phys. **A823**, 83(2009); J.-C. Wang, V. de la Incera, E. J. Ferrer and J. P. Keith, Phys. Rev. **D84**, 065014(2011); E. J. Ferrer and J. P. Keith, Phys. Rev. **C86**, 035205(2012).
- [18] B. O. Kerbikov, Phys. Atom. Nucl. **65**, 1918(2002); G. Sun, L. He and P. Zhuang, Phys. Rev. **D75**, 096004(2007); M. Kitazawa, D. H. Rischke and I. A. Shovkovy, Phys. Lett. **B663**, 228(2008); H. Abuki, G. Baym, T. Hatsuda and N. Yamamoto, Phys. Rev. **D81**, 125010(2010); H. Basler and M. Buballa, Phys. Rev. **D82**, 094004(2010); L. He, Phys. Rev. **D82**, 096003(2010); M. Matsuzaki, Phys. Rev. **D82**, 016005(2010).
- [19] Y. Nambu and G. Jona-Lasinio, Phys. Rev. **122**, 345(1961).
- [20] U. Vogl and W. Weise, Prog. Part. and Nucl. Phys. **27**, 195(1991); S. P. Klevansky, Rev. Mod. Phys. **64**(3), 649(1992); M. K. Volkov, Phys. Part. Nucl. **24**, 35(1993); T. Hatsuda and T. Kunihiro, Phys. Rep. **247**, 221(1994); M. Buballa, Phys. Rep. **407**, 205(2005).
- [21] A. Barducci, R. Casalbuoni, G. Pettini and L. Ravagli, Phys. Rev. **D71**, 016011(2005).
- [22] H. J. Warringa, D. Boer and J. O. Andersen, Phys. Rev. **D72**, 014015(2005).
- [23] K. Fukushima, K. Ohnishi, and K. Ohta, Phys. Rev. **C63**, 045203(2001).
- [24] B. Alles, M. D'Elia, and A. Di Giacomo, Nucl. Phys. **B494**, 281(1997).
- [25] M. Huang, P. Zhuang, and W. Chao, Phys. Rev. **D65**, 076012(2002).
- [26] P. Rehberg, S. P. Klevansky, and J. Hufner, Phys. Rev. **C53**, 410(1996).
- [27] P. Costa, M. C. Ruivo, C. A. de Sousa and Yu. L. Kalinovsky, Phys. Rev. **D71**, 116002(2005); Phys. Rev. **C70**, 025204(2004).
- [28] W. Detmold, K. Orginos, and Z. Shi, Phys. Rev. **D86**, 054507(2012).
- [29] It has been shown recently that this result is a consequence of the broken symmetry and is, therefore, exact. See A. Nicolis and F. Piazza, Phys. Rev. Lett. **110**, 011602(2013) and H.

Watanabe, T. Brauner, and H. Murayama, Phys. Rev. Lett. **111**, 021601(2013).
[30] L. He, Y. Jiang and P. Zhuang, Phys. Rev. **C79**, 045205(2009).

